Mechanical Systems and Signal Processing 169 (2022) 108787

Contents lists available at ScienceDirect

Mechanical Systems and Signal Processing

journal homepage: www.elsevier.com/locate/ymssp

Optimal sensor placement for parameter estimation and virtual sensing of strains on an offshore wind turbine considering sensor installation cost

Azin Mehrjoo [a], Mingming Song [a], Babak Moaveni [a,*], Costas Papadimitriou [b], Eric Hines [a]

[a] Tufts University, Medford, MA, USA
[b] University of Thessaly, Greece

ARTICLE INFO

Communicated by Laurent Mevel

Keywords:
Optimal sensor placement
Bayesian inference
Virtual sensing
Offshore wind turbines
Cost-information balance
Pareto optimal solution

ABSTRACT

This paper proposes an optimal sensor placement (OSP) framework for parameter estimation, virtual sensing, and condition monitoring using information theory. The framework uses a Bayesian OSP method combined with modal expansion to minimize the information entropy about quantities of interest (QoI), such as strain time histories at critical locations of the structure, without the knowledge of input excitation. The proposed optimization framework also accounts for variations in sensor installation cost at different locations on the monitored structure. The framework is evaluated numerically using a realistic model of an offshore wind turbine on a jacket support structure under installation cost assumptions and considering information entropy of the QoI. The QoI in this numerical study are considered to be the strain time history at one or more locations on the support structure in one problem and the parameters of the structure in the other. A correlation length is considered to account for the spatial correlation of data between adjacent sensors. Effects of the correlation length and input loads on the OSP results for parameter estimation are studied. The considered structural parameters for estimation in this study include (1) modulus of elasticity of tower elements (tower stiffness), (2) modulus of elasticity of jacket elements (jacket stiffness), and (3) vertical foundation spring (soil stiffness). The effect of a subjective weight between the information entropy and sensor configuration cost on the OSP results is also investigated. Different optimal designs are achieved for different weight factors, and the Pareto solutions for OSP are presented. It is found that the OSP framework is an effective tool for decision-makers considering the cost of instrumentation. The presented Pareto optimal solutions can give insight into the value of OSP given a limited budget.

1. Introduction

The global offshore wind energy (OWE) capacity is projected to expand 15-fold over the next two decades [1]. In light of our increasing dependence on this form of renewable energy, offshore wind developers, operators, and investors will benefit from stronger assurances of offshore wind turbines' (OWT) reliability through structural health monitoring (SHM). In addition to lowering investment risk, increased reliability can reduce the cost of maintenance and extend the design life of future wind farms. High-performance

* Corresponding author.

https://doi.org/10.1016/j.ymssp.2021.108787
Received 13 August 2021; Received in revised form 22 December 2021; Accepted 26 December 2021
Available online 7 January 2022

Nomenclature

$b(\mathbf{L})$	Normalized benefit
$c(\mathbf{L})$	Normalized cost
Cost_{ref}	Maximum cost for a specific number of sensors
$\mathbf{D} = \{\mathbf{y}_k \in R^{N_o}\}$	Sensor measurements
E_{jacket}, E_{tower}	Young's moduli of jacket and tower
$\mathbf{e}_k(\boldsymbol{\theta})$	Prediction error between model output and measurements
$f(w, \mathbf{L})$	Objective function
H	Information entropy
H_{max}	Maximum information entropy
H_{min}	Minimum information entropy
H_{ref}	Minimum information entropy for a specific number of sensors
$H_{z,prior}$	Information entropy before measuring data
$\mathbf{I}$	Identity matrix
k_L, k_V, k_R	Lateral, vertical, and rotational stiffness of soil
$\mathbf{L} \in R^{N_o \times N_d}$	Boolean matrix indicating location of measured DOFs
$\mathbf{L}^*$	Optimal sensor configuration
m	Number of contributing modes
N_d	Number of total DOFs in the model
N_o	Number of measured DOFs
N_z	Number of strain estimation location
N_θ	Size of θ
$\mathbf{Q}(\mathbf{L}\|\boldsymbol{\Sigma}_t, \widehat{\boldsymbol{\theta}}) \in R^{N_\theta \times N_\theta}$	Fisher Information Matrix
$\mathbf{q}_{m_k}$	Modal coordinate response at time step k
$\overline{\mathbf{q}}_k, \boldsymbol{\Sigma}_q$	Mean and covariance of posterior PDF of $\mathbf{q}_{m_k}$
$R(\delta_{ij})$	Spatial correlation function
s^2	Variance of sensor noise
u	Measure of OSP effectiveness
$U(\mathbf{L})$	Expected information gain
$u(\mathbf{L}, \mathbf{y})$	Utility function
w	Weight factor in objective function
$\mathbf{x}_k(\boldsymbol{\theta}) \in R^{Nd}$	Vector of predicted response at time step k
$\mathbf{y}_k \in R^{N_o}$	Measured response at time step k
$\mathbf{z}_k \in R^{N_z \times 1}$	Vector of predicted strains at time step k
$\overline{\mathbf{z}}_k, \boldsymbol{\Sigma}_z \in R^{N_z \times N_z}$	Mean and covariance of posterior PDF of $\mathbf{z}_k$
δ_{ij}	Spatial distance between measured DOFs
ε_k	Prediction error for strain estimation
$\widehat{\boldsymbol{\theta}}$	Vector of optimal values for parameters
$\boldsymbol{\theta} \in R^{N_\theta}$	Vector of structural parameters to be estimated
λ	Measure of spatial correlation length
$\boldsymbol{\Sigma}$	Covariance matrix of modeling error
$\overline{\boldsymbol{\Sigma}}$	Covariance matrix of measurement noise
$\boldsymbol{\Sigma}_t \in R^{N_o \times N_o}$	Covariance matrix of posterior PDF of $\mathbf{e}_k(\boldsymbol{\theta})$
$\boldsymbol{\Sigma}_{pr} \in R^{m \times m}$	Covariance matrix of prior PDF of $\mathbf{q}_{m_k}$
$\boldsymbol{\Sigma}_\varepsilon \in R^{N_z \times N_z}$	Covariance matrix of posterior PDF of $\boldsymbol{\varepsilon}_k$
$\boldsymbol{\Phi}_m(\mathbf{L}) \in R^{N_o \times m}$	Mode shape matrix for m contributing modes
$\boldsymbol{\Psi} \in R^{N_z \times m}$	Strain mode shape matrix for m contributing modes
$\nabla_{\boldsymbol{\theta}} = [\partial/\partial\theta_1 \quad \dots \quad \partial/\partial\theta_{N_\theta}]$	Gradient vector with respect to structural parameters

SHM consists of systematic monitoring and efficient condition-based maintenance strategies that are based on the right sensors in the right places for the right price, known as optimal sensor placement. Moreover, corrosion and fatigue are the most common failure mechanisms of an OWT support structure [2,3]. To evaluate the remaining life of such structures, it is necessary to know the level of stresses and strains over the life of the structure.

SHM implements damage identification strategies for engineering structures and estimating their remaining useful life. Damage refers to any variation of the mechanical properties of the structure over time. The techniques to estimate a structural system's mechanical properties from measurements are referred to as system identification methods. System identification methods can be

classified into output-only methods—where only the system's response is observed, and input–output methods—where the inputs and the response of the system are measured [4]. The objectives of SHM include investigation of uncertainties in structural behavior, condition-based maintenance, remaining lifetime prognosis, and optimization of future designs. In a rapidly growing global industry like OWE, these methods can help minimize Operation and Management (O&M) costs, protect against catastrophic failures, and provide feedback to improve the design of future turbines [5]. SHM methods can employ probabilistic Bayesian frameworks to account for uncertainties and errors in the measured data, estimation process, and structural model [6]. The application of Bayesian inference for SHM of civil structures was first introduced in 1998 [7]. Several studies include Bayesian inference applications for model updating and SHM of large-scale civil structures, which can be found in [8–13].

The reliability of an SHM procedure depends on the method's accuracy and the information available in the measured data. The location and type of sensors on the structure determine the level of information about the QoI in the data. SHM includes the experimental procedures to estimate a QoI using partially measured data [14]. Moreover, SHM includes virtual sensing, which is the process of estimating a QoI using a validated model and partially measured data. The experimental setup in SHM, corresponding to the number and location of the sensors, can be optimized to provide cost-effective and informative measurements about the QoIs [15]. This process is referred to as optimal sensor placement (OSP). This paper introduces an approach to OSP for estimating the parameters and strain history, and hence the fatigue life, of an OWT support structure. OSP methods hold promise for efficient condition-based monitoring at scale and could enable precise decision-making for entire OWT fleets regarding support structure maintenance and life extension.

Information theory-based approaches have been used by a number of researchers for OSP problems. These approaches can account for measurement uncertainties as well as modeling errors. Different measures of the information contained in the data were used to find the OSP solution. Some researchers have maximized the determinant or trace of the Fisher Information Matrix (FIM) [16–23], while others have employed the expected Bayesian loss function [24,25] to minimize the trace of the inverse of the FIM. A Bayesian framework for OSP in SHM applications was proposed in [26], where the OSP method optimized a metric related to the probability of damage detection of all regions of the structure. Shannon entropy [27], a measure of the uncertainty in model parameter estimation, was introduced in [28] for the OSP problem using a Bayesian framework. Shannon entropy is used in OSP for (i) parameter estimation when the input excitation is not measured [29], (ii) load identification of linear and nonlinear models [30], and (iii) model class selection for damage detection [31]. Shannon entropy depends on the determinant of the FIM for an asymptotically large number of data [15]. In [32], the expected information gain [33], which was derived from Kullback-Leibler divergence (KLD) [34], was maximized for finding OSP for response reconstruction. The effect of spatial correlation of the prediction error due to modeling error on the OSP problem was investigated in [35]. Estimating strains using virtual sensing is useful for fatigue estimation [40,41]. There are several studies in the literature using the modal expansion method for strain estimation of OWT [42–46]. Fatigue hotspots in an OWT with a jacket support structure are commonly underwater and difficult to access [47].

Solving the optimization problem of an OSP solution using discrete-valued design variables requires an exhaustive search over all the possible combinations of sensor types and locations. This is computationally expensive, even for a structure with a small number of degrees of freedom (DOFs). Heuristic algorithms such as Forward Sequential Sensor Placement (FSSP) and Backward Sequential Sensor Placement (BSSP) were proposed in [15,31], which overcome this computational problem but often provide a suboptimal sensor configuration. Genetic Algorithms [36–39] are alternatives for exhaustive search and can be used to complement FSSP and BSSP algorithms for improved results [35]; however, they are more computationally demanding than the heuristic algorithms.

Past OSP studies have not adequately explored the effect of cost on the OSP result. This paper investigates both single-objective optimization and multi-objective (Pareto efficiency) optimization to find OSP for the purpose of condition monitoring of an OWT for input–output parameter estimation and output-only strain estimation cases. The single-objective formulation minimizes the information entropy of the sensor configuration and does not consider the sensor configuration cost. The multi-objective OSP optimizes the cost-benefit objective function defined with different weight factors to balance the ratio of information and cost in the objective function. The present study suggests a balanced multi-objective OSP that provides insight into the effect of cost on the optimal sensor configuration.

The defined multi-objective function, Pareto study, and the application of the framework on OWT comprise the novelty of this work, where a combination of FSSP and BSSP search methods is used. The proposed method is called the 'combined sequential sensor placement' or SSP for short. The SSP gives near-optimal results comparable with the exhaustive search. Implementation of the algorithm is evaluated on optimal sensor configuration design of a realistic offshore wind turbine model for (1) parameter estimation and (2) strain estimation. The Pareto study presented in this paper provides insight to help decision-makers with the OSP design given a limited budget. A sensitivity analysis is performed to find the most influential parameters on the dynamical behavior of the structure and the selection of updating structural parameters. The study also considers the effect of spatially correlated prediction errors, which controls the minimum distance between sensors, as well as the effect of input excitation assumption on OSP results for parameter estimation in an input–output formulation. The effectiveness of the OSP algorithm is checked by comparing the best and worst configurations.

2. Methodology

This section presents the formulation of OSP for (1) parameter estimation and (2) strain estimation. Structural parameters of interest can include mass and/or stiffness of different components or substructures of a structure. In this study, the parameters reflecting the uncertainties in the model are modulus of elasticity of the tower, E_{tower}, modulus of elasticity of the jacket, E_{jacket}, and the vertical stiffness, k_v, of soil springs at the bottom of the jacket. These parameters are chosen based on a sensitivity analysis done on the structure. In the first two subsections, the Bayesian inference frameworks for each of these two purposes are briefly reviewed, and OSP

formulation using Shannon Entropy and Expected Utility is outlined afterward.

2.1. Bayesian inference framework for parameter estimation

The Bayesian inference framework for estimating unknown parameters of a structural model is briefly reviewed here. Assume $\boldsymbol{\theta} \in R^{N_\theta}$ be the vector of parameters of interest. Let $\mathbf{D} = \{\mathbf{y}_k \in R^{N_o}\}$ be the vector of measured acceleration response time history sampled over N points ($k = 1, .., N$) by Δt intervals where $\mathbf{y}_k \in R^{N_o}$ refer to output data and N_o is the number of measured DOFs, i.e., number of sensors. Let $\mathbf{x}_k(\boldsymbol{\theta}) \in R^{Nd}$ be the vector of predicted response time history from the Finite Element (FE) model at all DOFs (N_d) of the structure at each time step. The difference between the measurements and the model predictions is defined as the prediction error $\mathbf{e}_k(\boldsymbol{\theta})$, which includes the combined effects of modeling error and measurement noise. The relationship between the measured response $\mathbf{y}_k$ and $\mathbf{x}_k(\boldsymbol{\theta})$ follows Eq. (1):

$$\mathbf{y}_k = \mathbf{L}\mathbf{x}_k(\boldsymbol{\theta}) + \mathbf{e}_k(\boldsymbol{\theta}) \tag{1}$$

where $\mathbf{L} \in R^{N_o \times N_d}$ is a Boolean matrix consisting of ones at the measured DOFs and zeros elsewhere. It defines the number and location of sensors on the structure; therefore, it can be interpreted as the sensor configuration matrix. The prediction error is postulated to follow a Gaussian distribution with zero mean and covariance matrix $\boldsymbol{\Sigma}_t \in R^{N_o \times N_o}$. This assumption is justified by the principle of maximum information entropy, which states that the Gaussian distribution provides maximum uncertainty among all distributions with a specified mean and covariance. This imposes the least amount of constraint on the choice of distribution. However, other distributions can be assumed for the prediction error if there is prior knowledge about its statistical properties. Assuming prediction errors at different time steps are independent, the posterior probability density function (PDF) of the structural model parameters given the measured data has the following form [7]:

$$p(\boldsymbol{\theta}|\boldsymbol{\Sigma}_t, \mathbf{D}) \propto \frac{1}{(\sqrt{2\pi})^N \sqrt{det\boldsymbol{\Sigma}_t}} exp[-\frac{NN_o}{2} J(\boldsymbol{\theta}|\boldsymbol{\Sigma}_t, \mathbf{D})] p(\boldsymbol{\theta}) \tag{2}$$

where $p(\boldsymbol{\theta})$ is the prior PDF of updating parameters; and

$$J(\boldsymbol{\theta}|\boldsymbol{\Sigma}_t, \mathbf{D}) = \frac{1}{NN_o} \sum_{k=1}^{N} [\mathbf{y}_k - \mathbf{L}\mathbf{x}_k(\boldsymbol{\theta})]^{\mathrm{T}} \boldsymbol{\Sigma}_t^{-1} [\mathbf{y}_k - \mathbf{L}\mathbf{x}_k(\boldsymbol{\theta})] \tag{3}$$

represents the measure of fit between the measured data and corresponding model predictions. This method requires both the input and output of the system to evaluate the posterior PDF.

2.2. Bayesian inference framework for strain estimation

This section provides a review of the Bayesian inference framework and modal expansion technique for estimating strains at desired locations using measured time history structural response without the knowledge of input. Let $\mathbf{D} = \{\mathbf{y}_k \in R^{N_o}\}$ be the vector of displacement time history measurements where $\mathbf{y}_k$ is the output data at N_o DOFs and $\mathbf{e}_k$ be the Gaussian measurement error with zero mean and covariance matrix $\boldsymbol{\Sigma}_t \in R^{N_o \times N_o}$. The measured time history responses can be expanded using modal expansion formulation as:

$$\mathbf{y}_k = \boldsymbol{\Phi}_m(\mathbf{L})\mathbf{q}_{m_k} + \mathbf{e}_k \tag{4}$$

where $\boldsymbol{\Phi}_m(\mathbf{L}) \in R^{N_o \times m}$ is the mode shape matrix of m contributing modes at N_o DOFs and $\mathbf{q}_{m_k}$ is the modal coordinate vector of m contributing modes at time step k.

Subsequently, Bayesian inference is employed to estimate $\mathbf{q}_{m_k}$ and its uncertainty, i.e., posterior PDF of $\mathbf{q}_{m_k}$. Based on Bayes theorem, the posterior PDF of $\mathbf{q}_{m_k}$ given the measured time history $\mathbf{y}(t)$ is:

$$p(\mathbf{q}_{m_k}|\mathbf{y}_k) \propto p(\mathbf{y}_k|\mathbf{q}_{m_k})\ p(\mathbf{q}_{m_k}) \tag{5}$$

where $p(\mathbf{y}_k|\mathbf{q}_{m_k})$ is the likelihood function. Assuming the prior PDF $p(\mathbf{q}_{m_k})$ to be Gaussian with zero mean and covariance matrix $\boldsymbol{\Sigma}_{pr} \in R^{m \times m}$, the posterior PDF of $\mathbf{q}_{m_k}$ is Gaussian with $\overline{\mathbf{q}}_k$ mean and $\boldsymbol{\Sigma}_q$ covariance [32,48,49] given by

$$\overline{\mathbf{q}}_k = \left[\boldsymbol{\Phi}_m^{\mathrm{T}}(\mathbf{L})\boldsymbol{\Sigma}_t^{-1}(\mathbf{L})\boldsymbol{\Phi}_m(\mathbf{L}) + \boldsymbol{\Sigma}_{pr}^{-1}\right]^{-1} \boldsymbol{\Phi}_m^{\mathrm{T}}(\mathbf{L})\boldsymbol{\Sigma}_t^{-1}(\mathbf{L})\mathbf{y}_k \tag{6}$$

$$\boldsymbol{\Sigma}_q(\mathbf{L}) = \left[\boldsymbol{\Phi}_m^{\mathrm{T}}(\mathbf{L})\boldsymbol{\Sigma}_t^{-1}(\mathbf{L})\boldsymbol{\Phi}_m(\mathbf{L}) + \boldsymbol{\Sigma}_{pr}^{-1}\right]^{-1} \tag{7}$$

The modal expansion technique is then employed for virtual sensing, i.e., to predict strains at the desired DOFs. This can be done using the estimated modal coordinate and assuming a Gaussian prediction error with zero mean and covariance $\boldsymbol{\Sigma}_\varepsilon \in R^{N_z \times N_z}$:

$$\mathbf{z}_k = \boldsymbol{\Psi}\mathbf{q}_{m_k} + \boldsymbol{\varepsilon}_k \tag{8}$$

where $\mathbf{z}_k \in R^{N_z \times 1}$ is the vector of predicted strains at desired locations (N_z) and $\boldsymbol{\Psi} \in R^{N_z \times m}$ is the strain mode shape matrix of m contributing modes.

By propagating the uncertainty of estimated $\mathbf{q}_{m_k}$ to $\mathbf{z}_k$ in Eq. (8), $\mathbf{z}_k$ follows a Gaussian distribution with $\bar{\mathbf{z}}_k$ mean and $\boldsymbol{\Sigma}_z \in R^{N_z \times N_z}$ covariance given by:

$$\bar{\mathbf{z}}_k = \boldsymbol{\Psi}\left[\boldsymbol{\Phi}_m^{\mathrm{T}}(\mathbf{L})\boldsymbol{\Sigma}_t^{-1}(\mathbf{L})\boldsymbol{\Phi}_m(\mathbf{L}) + \boldsymbol{\Sigma}_{pr}^{-1}\right]^{-1}\boldsymbol{\Phi}_m^{\mathrm{T}}(\mathbf{L})\boldsymbol{\Sigma}_t^{-1}(\mathbf{L})\mathbf{y}_k \tag{9}$$

$$\boldsymbol{\Sigma}_z(\mathbf{L}) = \boldsymbol{\Psi}\left[\boldsymbol{\Phi}_m^{\mathrm{T}}(\mathbf{L})\boldsymbol{\Sigma}_t^{-1}(\mathbf{L})\boldsymbol{\Phi}_m(\mathbf{L}) + \boldsymbol{\Sigma}_{pr}^{-1}\right]^{-1}\boldsymbol{\Psi}^{\mathrm{T}} + \boldsymbol{\Sigma}_\varepsilon \tag{10}$$

Eq. (10) indicates that the uncertainty in estimated strains does not depend on the measurements $\mathbf{y}_k$. Consequently, optimal sensor placement for strain estimation, which relies on minimizing a scalar measure of $\boldsymbol{\Sigma}_z$, does not directly require the input or output measurements.

The strain mode shape matrix is a property of the structure and can be calculated utilizing the displacement mode shape matrix and shape functions used in the FE model (for example, Hermitian shape function for beam-column element).

2.3. Spatial correlation of prediction error

In this study, the effect of spatial correlation of prediction errors between neighboring DOFs is considered. The covariance of total prediction error should accord with the errors and correlations inhere in the measurements and the model. However, no measurements are available during the sensor design stage. In [35], the authors used a measure of spatial correlation length and assumed an exponential correlation function to consider the effect of spatially correlated prediction error. This procedure is briefly introduced here. Considering independency between measurement noise and modeling error, the total prediction error matrix $\boldsymbol{\Sigma}_t$ takes the form:

$$\boldsymbol{\Sigma}_t = \overline{\boldsymbol{\Sigma}} + \boldsymbol{\Sigma} \tag{11}$$

where $\overline{\boldsymbol{\Sigma}}$ and $\boldsymbol{\Sigma}$ are the covariance matrices of the measurement noise and modeling error, respectively. As measurement noise is independent of the location of the sensors, $\overline{\boldsymbol{\Sigma}} = s^2\mathbf{I}$ is considered as a diagonal matrix where $\mathbf{I}$ is the identity matrix and s^2 denotes the variance of sensor noise. However, due to the correlation between neighboring locations because of modeling error, the covariance matrix $\boldsymbol{\Sigma}$ can have non-zero off-diagonal terms. The correlation between the prediction errors at DOFs i and j is assumed to be:

$$\Sigma_{ij} = \sqrt{\Sigma_{ii}\Sigma_{jj}}R(\delta_{ij}) \tag{12}$$

where R is a function of δ_{ij}, which is the spatial distance between the DOFs. The same correlation function as [35] is used in this study:

$$R(\delta_{ij}) = exp[-\delta_{ij}/\lambda] \tag{13}$$

where λ is a measure of the spatial correlation length, and a larger value λ assigns a stronger correlation to distant DOFs. The correlation length λ should be chosen such that the covariance matrix in Eq. (12) be consistent with the actual errors and correlations as observed from measurements. However, no such measurements are available in the design phase. The correlation length is recommended to be significantly smaller than the "wavelength" of the highest contributing mode. In [35], it is shown that for up to the characteristic length of the highest contributing mode of the structure, the spatial correlation between prediction errors forces the minimum distance between sensors to be of the order of the correlation length.

2.4. Optimal sensor placement formulation

The information entropy method has been used in this study for OSP. For parameter estimation, the formulation is derived using the definition of information entropy and asymptotic approximation. For strain estimation, KLD, expected information gain and information entropy are used. In general, information entropy is a scalar measure of uncertainty associated with a QoI, and information gain is the reduction in uncertainty about the QoI after measuring data. Optimizing either measure would lead to the same optimal experimental setup.

2.4.1. OSP framework for parameter estimation

For the purpose of parameter estimation, the information entropy H is defined as:

$$H(\mathbf{L}|\boldsymbol{\Sigma}_t, \mathbf{D}) = E_{\boldsymbol{\theta}}(-lnp(\boldsymbol{\theta}|\boldsymbol{\Sigma}_t, \mathbf{D})) = -\int lnp(\boldsymbol{\theta}|\boldsymbol{\Sigma}_t, \mathbf{D})p(\boldsymbol{\theta}|\boldsymbol{\Sigma}_t, \mathbf{D})d\boldsymbol{\theta} \tag{14}$$

which depends on measured data $\mathbf{D}$ and sensor configuration $\mathbf{L}$. $E_{\boldsymbol{\theta}}(\ldots)$ denotes mathematical expectation with respect to vector $\boldsymbol{\theta}$. Minimizing the entropy would result in OSP. For uninformative (i.e., uniform) prior PDF of the model parameters, the information entropy can be asymptotically approximated when a large amount of data is available [15]:

$$H(\mathbf{L}|\boldsymbol{\Sigma}_t,\mathbf{D}) = \frac{1}{2}N_{\boldsymbol{\theta}} ln(2\pi) - \frac{1}{2} ln[det\mathbf{Q}(\mathbf{L}|\boldsymbol{\Sigma}_t,\widehat{\boldsymbol{\theta}})] \tag{15}$$

where $\widehat{\boldsymbol{\theta}}$ is the vector of optimal values for the parameters and $\mathbf{Q}(\mathbf{L}|\boldsymbol{\Sigma}_t,\widehat{\boldsymbol{\theta}}) \in R^{N_\theta \times N_\theta}$ is the FIM which contains information about the uncertainty of estimated parameters, given by:

$$\mathbf{Q}(\mathbf{L}|\boldsymbol{\Sigma}_t,\widehat{\boldsymbol{\theta}}) = \sum_{k=1}^{N} (\mathbf{L}\nabla_{\boldsymbol{\theta}}\mathbf{x}_k(\widehat{\boldsymbol{\theta}}))^{\mathrm{T}} \left(\mathbf{L}\boldsymbol{\Sigma}_t\mathbf{L}^{\mathrm{T}}\right)^{-1} (\mathbf{L}\nabla_{\boldsymbol{\theta}}\mathbf{x}_k(\widehat{\boldsymbol{\theta}})) \tag{16}$$

in which $\nabla_{\boldsymbol{\theta}} = \left[\, \partial/\partial\theta_1 \quad \ldots \quad \partial/\partial\theta_{N_\theta} \,\right]$ is the gradient vector with respect to the parameter vector $\boldsymbol{\theta}$. The FIM in Eq. (16) is created using the sensitivities of response in sensor locations with respect to the model parameters to be inferred. The logarithm of the determinant of FIM which is present in Eq. (15) is an overall scalar measure of this sensitivity. In the absence of experimental data, the optimal value $\widehat{\boldsymbol{\theta}}$ of the model parameter set is not available. To proceed with the optimal design, the value of $\widehat{\boldsymbol{\theta}}$ is assigned a nominal value. The nominal value of the parameters is considered as the true value of model parameters to represent the actual structural system. The uncertainty in the nominal value $\widehat{\boldsymbol{\theta}}$ can be considered by using the expected information entropy over all possible values $\widehat{\boldsymbol{\theta}}$ quantified by the prior probability distribution $p(\widehat{\boldsymbol{\theta}})$.

2.4.2. OSP framework for strain estimation

Optimal sensor placement for strain estimation is formulated using the expected information gain $U(\mathbf{L})$ [50]:

$$U(\mathbf{L}) = \int_{\Upsilon} u(\mathbf{L},\mathbf{y}) p(\mathbf{y}|\mathbf{L}) d\mathbf{y} \tag{17}$$

where $u(\mathbf{L},\mathbf{y})$ is the utility function using the KLD between the prior and posterior probability distribution of the response QoI $\mathbf{z}_k$ introduced in Eq. (8). KLD measures the amount of information added to the prior after measuring the data. This scalar value shows the usefulness of the experimental design. Maximizing this measure would result in the OSP. In [50], it is shown that Eq. (17) can be rewritten in terms of the change in information entropy after measuring the data by:

$$U(\mathbf{L}) = H_{z,prior} - \int_{\Upsilon} H_z(\mathbf{L},\mathbf{y}|\mathbf{D}) p(\mathbf{y}|\mathbf{L}) d\mathbf{y} \tag{18}$$

where $H_{z,prior}$ is the information entropy before measuring data and $H_z(\mathbf{L},\mathbf{y}|\mathbf{D})$ is information entropy after measuring data. Following the fact that the QoI $\mathbf{z}_k$ is Gaussian distributed with covariance matrix $\boldsymbol{\Sigma}_z(\mathbf{L})$ in Eq. (10) that does not depend on the data $\mathbf{y}$, the information entropy for the response QoI $\mathbf{z}_k$ takes the form [32]:

$$H_z(\mathbf{L},\mathbf{y}|\mathbf{D}) = H_z(\mathbf{L}|\mathbf{D}) = \frac{1}{2}N_z[ln(2\pi)+1] + \frac{1}{2} ln(det(\boldsymbol{\Sigma}_z(\mathbf{L}))) \tag{19}$$

which is independent of the data $\mathbf{y}$. Using this independence of the posterior information entropy $H_z(\mathbf{L},\mathbf{y}|\mathbf{D}) = H_z(\mathbf{L}|\mathbf{D})$ on the data $\mathbf{y}$, the integral in (18) simplifies to $U(\mathbf{L}) = H_{z,prior} - H_z(\mathbf{L}|\mathbf{D})$. Considering that the prior information entropy $H_{z,prior}$ is constant and independent of the sensor configuration, minimizing posterior information entropy $H_z(\mathbf{L}|\mathbf{D})$ is the mathematical counterpart of maximizing information gain. This study's objective is to find a sensor configuration $\mathbf{L}$ that minimizes the posterior information entropy $H_z(\mathbf{L}|\mathbf{D})$ for predicting strains at desired hotspot locations.

The optimal sensor configuration assures that no other setup could result in a more informative observation. It is worth noting that the information entropy presented in Eq. (15) for parameter estimation and Eq. (19) for strain estimation do not directly depend on the sensor measurements ($\mathbf{y}_k$) but sensor locations ($\mathbf{L}$). This is ideal for the instrumentation design phase, where no measurements are yet available.

The following metric is also defined to measure the effectiveness of the OSP

$$u = \frac{H_{max} - H_{min}}{H_{min}} \tag{20}$$

where H_{max} and H_{min} are maximum and minimum information entropies corresponding to the worst and best sensors configurations. A small value of u (close to zero) indicates that the best and worst sensor configurations provide a similar level of information; thus, an OSP process is not beneficial for the problem, and the higher this measure, the more beneficial the OSP algorithm.

2.5. Consideration of sensor configuration cost

The cost of sensor configuration is considered using an objective function with a weight factor to balance the benefit of minimizing the information entropy and the cost of sensor configuration. The cost and information entropy values are not in the same order of magnitude, and therefore their values are normalized in the objective function. Two reference terms H_{ref} and Cost_{ref} are defined as the minimum information entropy and maximum cost obtained by assuming a certain number of sensors (e.g., eight sensors in this study). The benefit term for each sensor configuration $H(\mathbf{L})$ is normalized by H_{ref} and the cost term $\text{Cost}(\mathbf{L})$ is normalized by Cost_{ref}. The

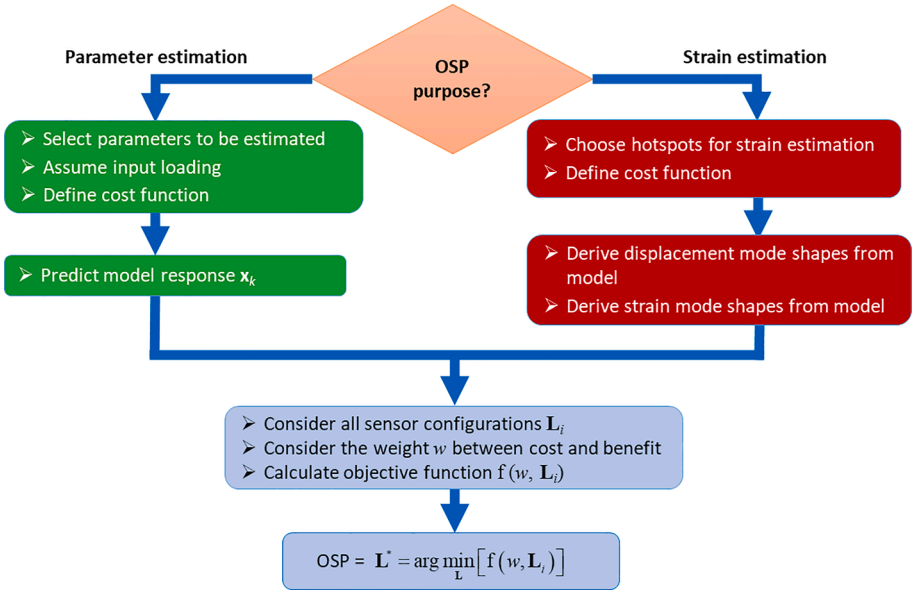

Fig. 1. The OSP procedure framework.

information entropy is a decreasing function of the number of the sensors, and the normalized benefit could be controlled by H_{ref} which refers to the minimum entropy for a reference number of sensors. This normalization will not affect the results and only makes the values of the weight factors more reasonable. $H(\mathbf{L})$ is used for notation brevity for posterior information entropy instead of $H(\mathbf{L}|\boldsymbol{\Sigma}_t, \mathbf{D})$ for parameter estimation and $H_z(\mathbf{L}|\mathbf{D})$ for strain estimation. It should be noted that cost value is always between zero and one, and benefit values are always positive.

$$\begin{cases} b(\mathbf{L}) = \left(H(\mathbf{L}) - H_{ref}\right)/H_{ref} \\ c(\mathbf{L}) = \mathrm{Cost}(\mathbf{L})/\mathrm{Cost}_{ref} \end{cases} \tag{21}$$

where sensor configuration cost is defined by a cost function, including sensor cost, which is constant, and installation costs which is variable for different locations, a non-uniform installation cost is considered for different locations, as is the case for OWTs. The cost-benefit objective function is defined in Eq. (22). The weight factor w in this equation defines the relative importance of information entropy versus cost.

$$\begin{cases} \mathrm{f}(w, \mathbf{L}) = w \times b(\mathbf{L}) + (1 - w) \times \mathrm{c}(\mathbf{L}) \\ \mathbf{L}^* = \underset{\mathbf{L}}{argmin}[f(w, \mathbf{L})] \end{cases} \tag{22}$$

A Pareto front study is performed considering varying weights between cost and information entropy. An advantage of the proposed formulation is that it offers the ability to use approximate numerical methods over an expensive exhaustive search. A simplified diagram for the OSP framework is presented in Fig. 1.

2.6. Computational algorithm for OSP

Consider a structure with N_d DOFs that is going to be instrumented with N_o sensors. The total number of sensor configurations on this structure is

$$\binom{N_d}{N_o} = \frac{N_d!}{N_o!(N_d - N_o)!} \tag{23}$$

which for practical cases is a considerably large number. Finding the optimal sensor configuration among this set requires an exhaustive search, which is computationally expensive. There are two computationally efficient approximate alternative approaches to solve this problem, namely the FSSP and the BSSP algorithms, which provide near-optimal solutions. In the FSSP approach, the sensors' position is chosen sequentially by placing one sensor in the location that results in the highest decrease in information entropy. Specifically, given that i-1 sensors have been placed on the structure, the position for the i^{th} sensor is determined among $N_d - i + 1$ possible locations. Starting with $i = 1$, this process continues until the total number of desired sensors is reached. This approach can also be used in a backward manner (BSSP). In the application of BSSP, the algorithm starts with N_d sensors placed at all of the structure's DOFs, and then sensors are removed one by one from the location resulting in the smallest increase of the information entropy until the desired number of sensors is achieved. It is worth noting that the FSSP and BSSP only provide the optimal solution

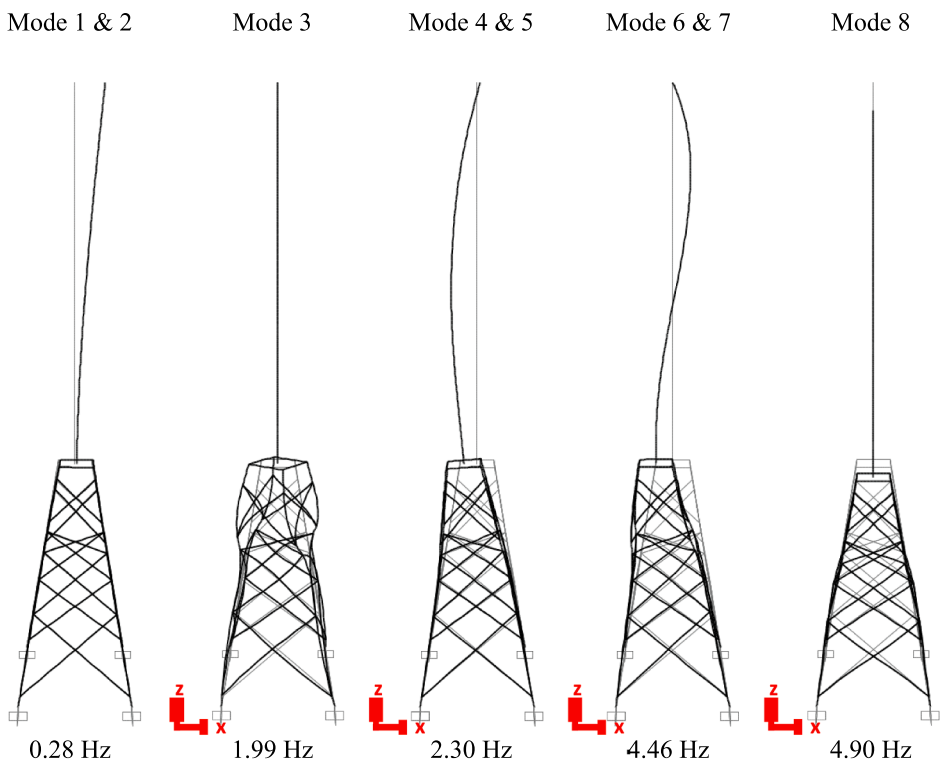

Fig. 2. The contributing modes of the structure.

when the optimal sensor configuration for an i-sensor configuration is a subset of an $i+1$-sensor configuration. However, the resultant information entropy using these algorithms is demonstrated to be close to the absolute optimal sensor configuration [35]. The FSSP approach needs $\sum_{i=1}^{N_o}(N_d-i+1)$ optimization iterations, and BSSP needs $\sum_{i=1}^{N_d-N_o+1}(N_d-i+1)$ optimization iterations, which are much smaller than the number required by the exhaustive search.

In this paper, a combined SSP approach is used for OSP. In this approach, for a given number of sensors, a simultaneous FSSP and BSSP search is done. Later, the information entropies for the resultant configurations are compared, and the configuration with lower information entropy is chosen as the optimal configuration. The combined SSP approach is found to perform better than FSSP or BSSP and provides very accurate results which are close to those obtained by exhaustive search.

3. Description of the OWT model

The case study structure in this paper is a numerical model of an offshore wind turbine on a jacket support structure based on a real offshore wind turbine. A linear elastic FE model of this wind turbine was created using the structural analysis software OpenSees [51]. The tower was modeled using 32 beam elements with varying cross-sections, and an assumed concentrated mass of 500 tons at the top representing the rotor-nacelle assembly (RNA). The masses of tower and jacket elements were lumped at their end nodes. The modulus of elasticity was assumed to be 200 GPa for the steel material, which was used for all elements. A rotational mass of 1.8×10^7 kg-m^2 was assigned at the top of the tower for RNA mass moment of inertia about X and Y axes (see Fig. 2 for axis orientations). The soil-structure interaction was modeled using three linear springs at the bottom of the four jacket legs, i.e., k_L, k_V, and k_R. The lateral stiffness of soil constraint (k_L) was assumed to be the same in X and Y directions, and the vertical stiffness (k_V) and rotational constraint (k_R) are assumed to be the same for four legs.

The presented OSP framework is applied on a realistic but simple numerical model to demonstrate the OSP process on an OWT. In the simplification of the model, the following OWT complexities are not considered: asymmetry of RNA, the effect of the rotor on dynamics of the structure, distributed wind load along the height of the structure, wave loads, and wave/wind misalignment. However, the framework can be applied to a more detailed model and loading conditions.

Fig. 2 shows the natural frequencies and mode shapes of the OWT. Due to the symmetry of the structure, modes 1 & 2 and 4 & 5 have the same natural frequencies and similar mode shapes in X and Y directions, respectively, while the third mode is torsional. All mode shapes except for mode 3 have relatively large deformations at mid-height of the tower.

In the application of OSP for parameter estimation, the following considerations have been taken into account for the selection of updating model parameters: (1) the number of updating parameters should not get too large, so the inverse updating problem is observable, (2) model parameters with considerable prior uncertainty such as foundation stiffness should be considered, (3)

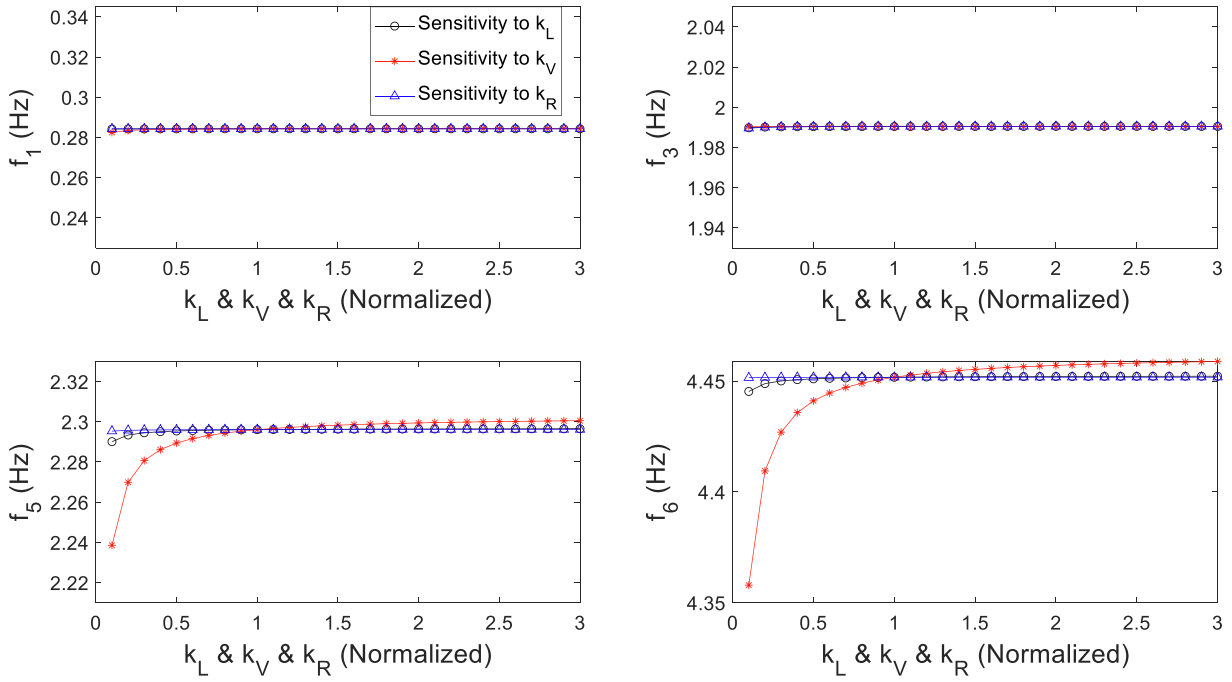

Fig. 3. Sensitivity analysis results with respect to the stiffness of soil constraints.

parameters should have sensitivity to measurements, and (4) selected updating parameters must be able to compensate for unmodeled components and modeling errors.

A sensitivity analysis is performed on the three foundation springs (k_L, k_V, and k_R) to study their influence on dynamic properties (natural frequencies) of the OWT. Fig. 3 shows the sensitivity of natural frequencies of modes 1, 3, 5, and 6 with respect to the soil springs. The values of springs have been normalized to their initial values, which are 42.66 GN/m for k_L & k_V and 136.04 GN-m/rad for k_R. These initial values are based on soil constraints used for an offshore wind turbine in the North Sea [40]. It can be observed that only the higher modes (fifth and sixth) natural frequencies are affected by the vertical spring k_V, while k_L and k_R have little effect on any of the vibration modes considered. Therefore, only vertical spring stiffness for the foundation is considered as an updating parameter.

Furthermore, the OWT structure is divided into two substructures with two updating parameters representing their moduli of elasticity: E_{jacket} for all elements in the jacket and E_{tower} for the tower. The moduli of elasticity are influential on the dynamic response and can potentially compensate for modeling errors at different parts of the structure. Therefore, the final updating parameters are $\boldsymbol{\theta} = [E_{jacket}, E_{tower}, k_v]^{\mathrm{T}}$.

4. OSP results for parameter estimation

This section describes the results of OSP for parameter estimation for the considered OWT and studies the effects of data correlation, input loads, and numerical optimization algorithms on OSP results. Due to the symmetry of the structure, only X-direction DOFs are considered as possible sensor measurements. This assumption reduces the computational cost, especially for the exhaustive search.

4.1. Effects of data correlation

In this section, the importance of considering the spatial correlation between measurements caused by prediction errors on the OSP result is studied. Results of OSP are presented and compared for two cases where data correlation is considered or not. The prior distribution of updating parameters is assumed to be uniform.

The OSP is performed for estimating $\boldsymbol{\theta} = [E_{jacket}, E_{tower}, k_v]^{\mathrm{T}}$ considering up to ten sensors. Due to the computational efficiency of SSP and its accuracy, this numerical approach is used to solve the optimization problem iteratively. The sensors' order is an indicator of their relative importance in gaining information and reducing uncertainty about the updating parameters. Fig. 4a shows the OSP result for the case when no data correlation is considered. The results show that 4 out of 5 sensors are clustered in the middle of the tower, which is justified considering the structure's dominant mode shapes have larger amplitudes in the middle of the tower, as shown in Fig. 2. However, sensors placed at adjacent nodes of the finite element mesh may provide redundant information. This approach clearly ignores the correlation between the data acquired in neighboring locations, which is not a realistic assumption.

In order to address this issue, a spatial correlation length of prediction errors may be considered. The spatial correlation length can

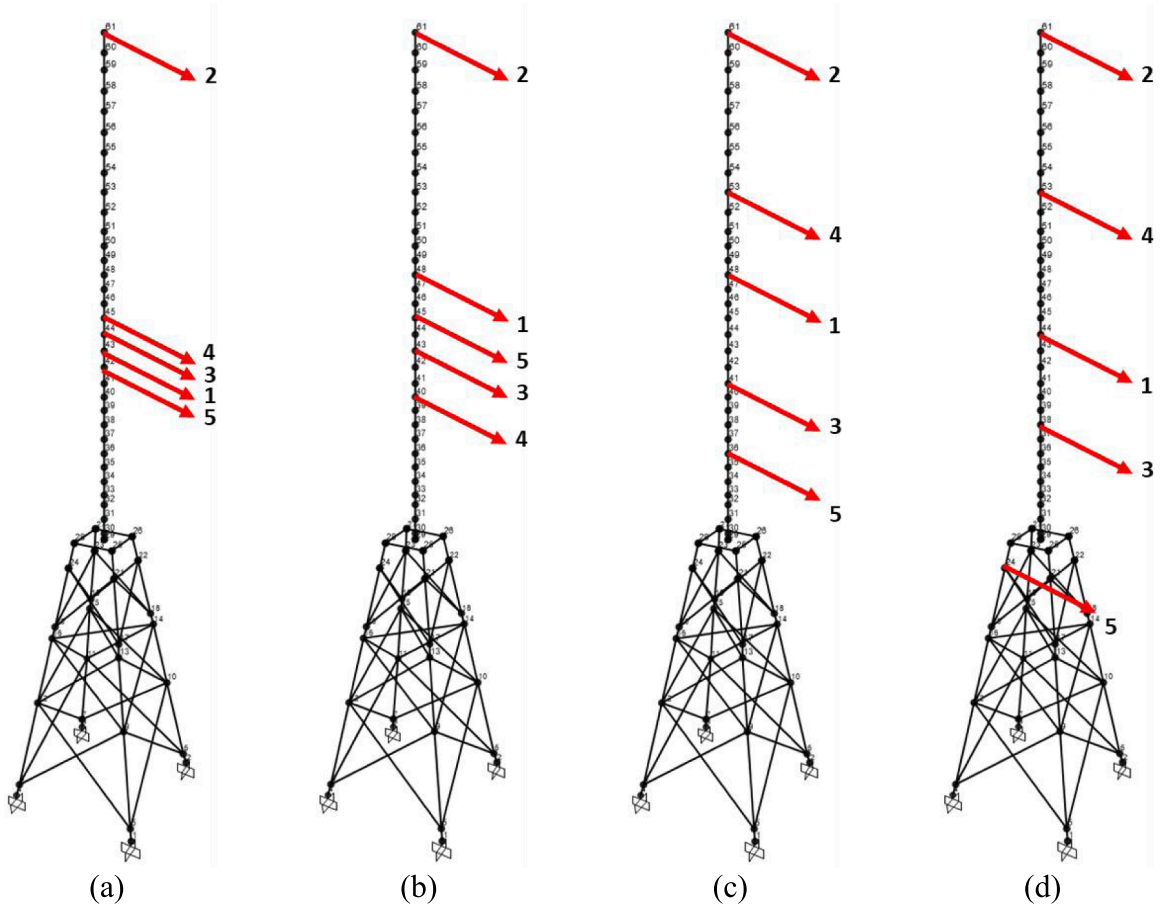

Fig. 4. OSP results: (a) no correlation is considered; (b) $\lambda = 2$; (c) $\lambda = 5$; and (d) $\lambda = 10$.

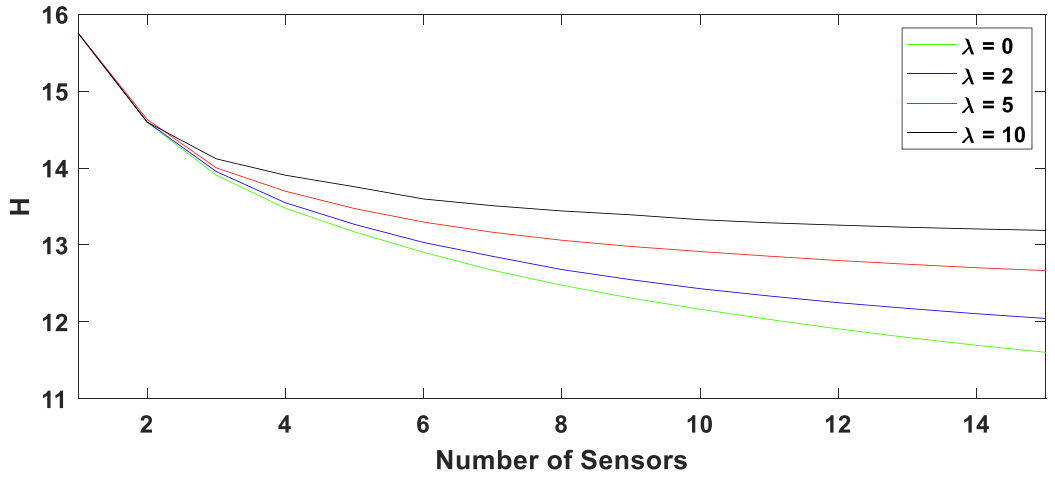

Fig. 5. Relative information entropy comparison.

be accounted for in the covariance matrix of the total prediction error, as shown in Eq. (13). To investigate the effect of correlation length, given the number of $N_o = 5$ sensors, OSP analysis is performed for $\lambda = 2,5,10$. The correlation length controls the correlation among neighboring DOFs, and a larger correlation length indicates a correlation between farther DOFs, and therefore, the optimal sensors' locations would be more spread out. The results for $\lambda = 2, 5, 10$ are shown in Fig. 4b–d, respectively. The red arrows in all the corresponding figures in this paper are an indicator of the location and direction of the measurements. It can be seen that the optimal

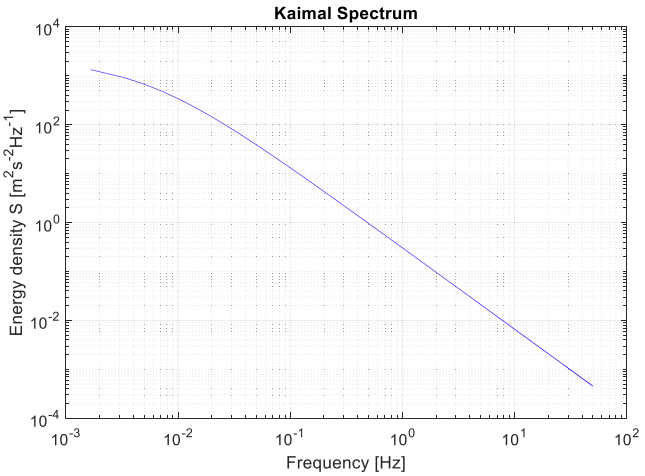

Fig. 6. The Kaimal spectrum.

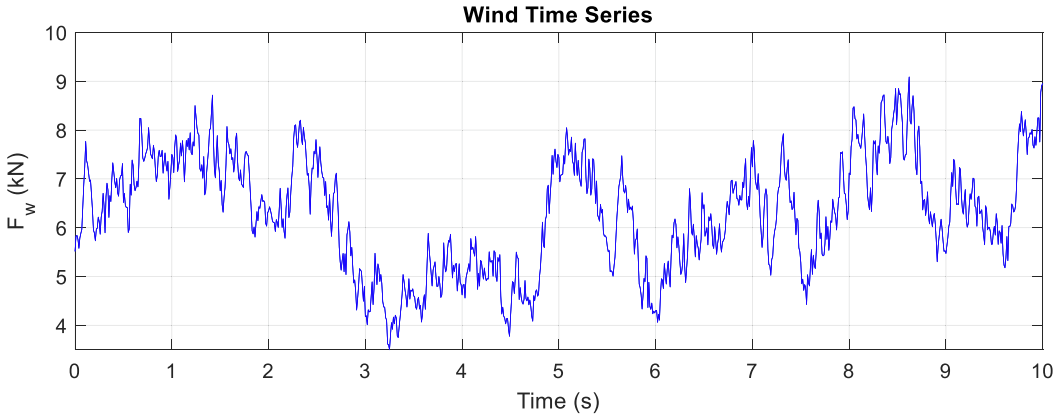

Fig. 7. Time history of the lateral wind load.

sensor locations get farther away from each other by increasing the correlation length measure. While the correlation between sensors exists, a large correlation length may also be unrealistic. In the lack of measurement correlation consideration, OSP results depend on the finite element discretization as the sensors would be placed in adjacent nodes.

Fig. 5 shows the information entropy versus the number of sensors for different spatial correlation lengths. It can be seen that more than 80 percent of the information entropy reduction can be obtained by optimally placing six sensors, and the reduction becomes less significant as the number of sensors increases. Moreover, increasing the spatial correlation length results in higher information entropy. This increase in entropy is reasonable since the correlation length adds a constraint in sensor placement and reduces the total amount of information by implying that some measurements are correlated.

4.2. *Effects of input loads*

OSP for parameter estimation in this paper is formulated assuming known input excitation. The input load is required to simulate the model-predicted response ($\mathbf{x}_k$) in Eq. (16). In this section, the sensitivity of OSP results to different input load assumptions is demonstrated. Two different loading conditions on the OWT are considered: (1) only lateral load and (2) a combination of lateral and torsional loads. Both loads are assumed as resultant point loads and applied at the top of the structure (nacelle level). The Kaimal spectrum [52] is used as an approximation of the wind power spectrum. Fig. 6 shows the Kaimal spectrum with a mean wind speed of 10 m/s and a standard deviation of 4. The simulated wind load time history is depicted in Fig. 7. The torsional load is also assumed to follow the same Kaimal spectrum, and its time history is simulated using the lateral load time history multiplied by a factor of 4.

The analysis is performed assuming $N_o = 10$ (number of sensors) and $\lambda = 5$ (correlation length). The results are shown in Fig. 8. It can be observed that the input loads can significantly affect the optimal sensor configurations. More sensors are placed on the jacket when the torsional load is present, which is reasonable as the torsional response of the structure is mainly represented by the torsional movement of the jacket (see mode shape 3 in Fig. 2). Moreover, in this case study, the tower is modeled as a cantilever beam, and thus

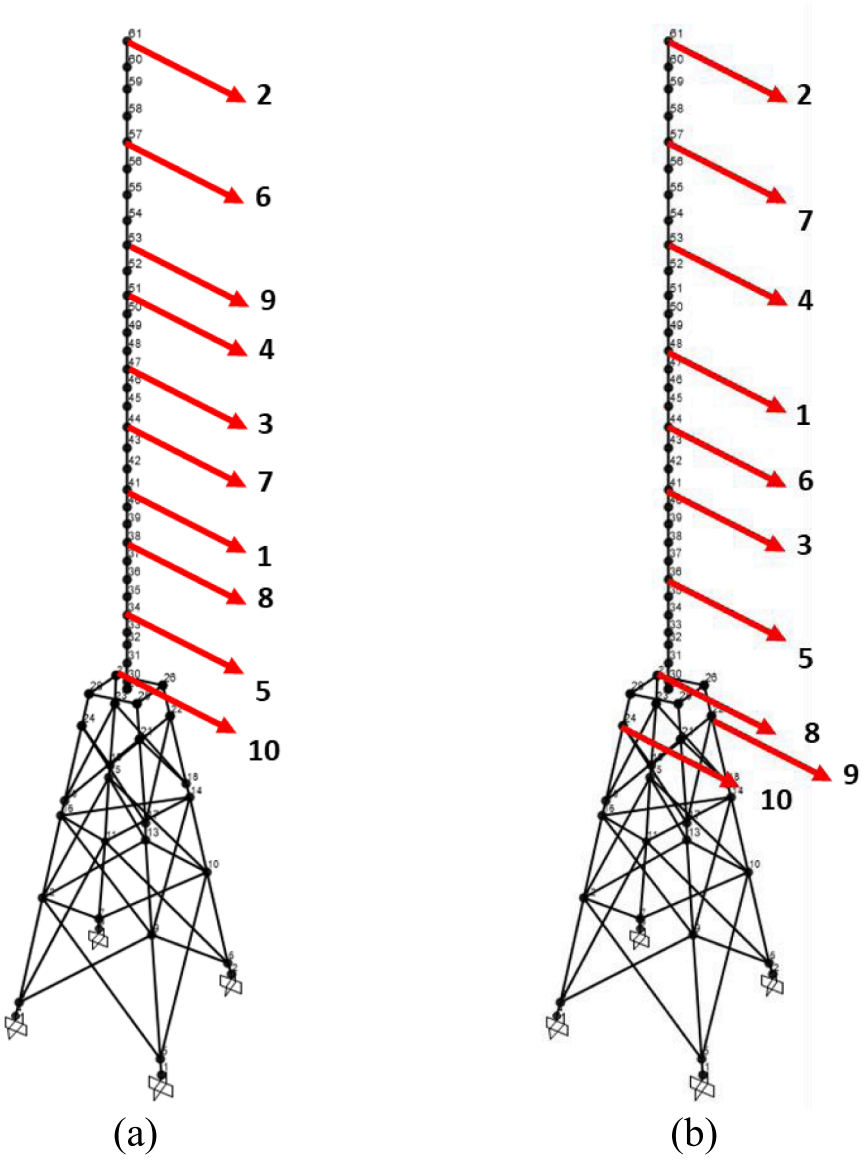

Fig. 8. OSP results considering (a) lateral load; (b) a combination of lateral and torsional load.

the sensor on the tower cannot capture torsional motion. The location of the first couple of sensors which are the most informative ones, varies for different input loads. This means that input loads directly affect the OSP results.

4.3. Comparing SSP and exhaustive search

There are several search algorithms available to find the OSP configuration, including FSSP, BSSP, and the exhaustive search. Only the exhaustive search method guarantees the optimal solution as all combinations of sensor configurations are considered and compared. However, this method is computationally expensive. The alternative search method which is used in this study is the SSP method which combines the results of FSSP and BSSP methods at each iteration. In this section, results of OSP using SSP and exhaustive search are compared under the combined torsional and lateral input loads for 1-sensor to 5-sensor configurations. A spatial correlation length of $\lambda = 5$ is assumed. Fig. 9 depicts the sorted information entropy of all configurations using the exhaustive search for a total of 4.613029×10^6 configurations along the X-axis. The red dots in Fig. 9 show the information entropy of the optimal configuration for all the configurations of 1–5 sensors. In this plot, it can be observed that entropy can be drastically reduced by changing sensor locations and thus highlighting the value of OSP. Increasing the number of sensors results in lower optimal information entropy, which is expected. However, the information entropy for optimal configuration of 3, 4, and 5 sensors are very close. Fig. 10 presents the OSP results for parameter estimation for 1–5 sensor configurations. The results show that the information provided by only lateral

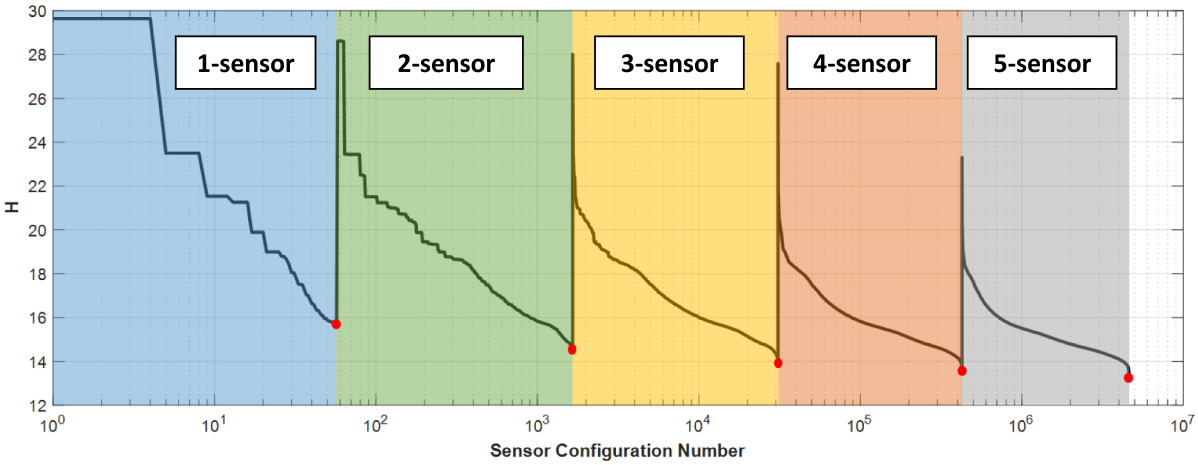

Fig. 9. Sorted information entropy for 1–5 sensor configurations.

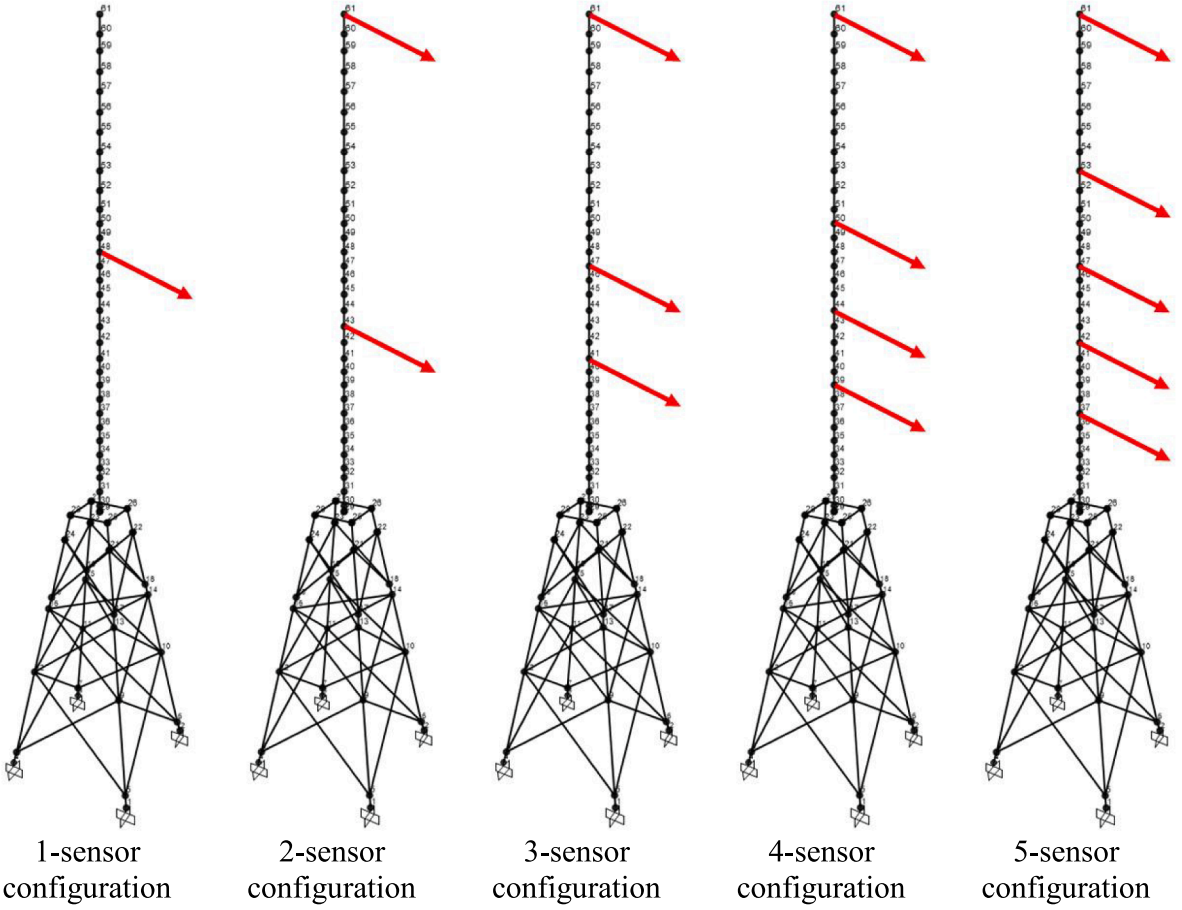

Fig. 10. Optimal sensor configuration results corresponding to each specific sensor number.

measurements is adequate for estimating the three parameters of interest. This would not be the case if only torsional motion provided unique information about a parameter of interest. For example, if the estimation of the soil spring under only one leg or the stiffness of a single diagonal truss member of the jacket was sought after. Fig. 11 compares the accuracy of the SSP method to the exhaustive

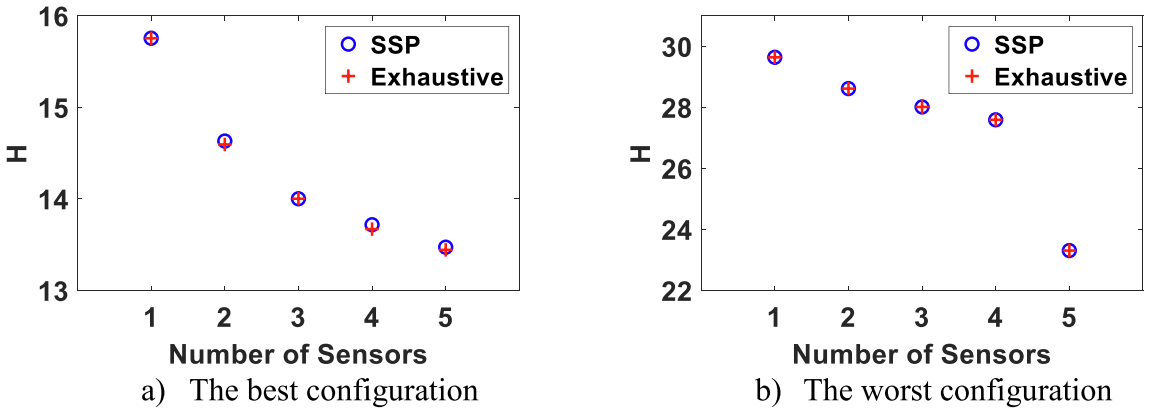

Fig. 11. Comparing information entropy of optimal configurations using SSP and exhaustive search methods.

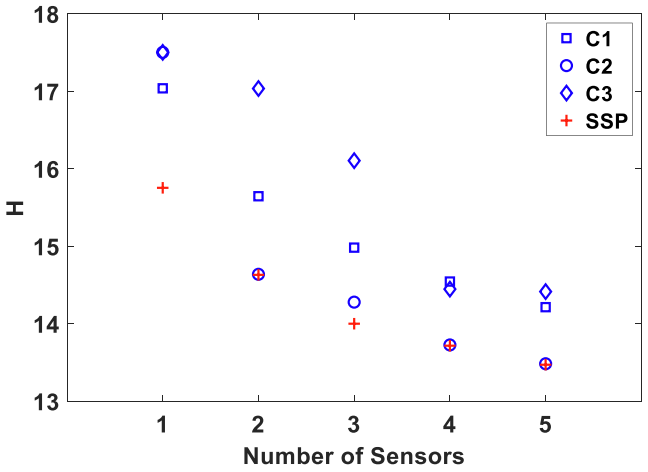

Fig. 12. Information entropy of the best and the worst configurations compared for SSP and exhaustive search.

search. In Fig. 11, the information entropy for the best and worst configurations and for the 1–5 sensor configurations are compared using two search methods. The results are almost identical, confirming the accuracy of the SSP method.

Results of the OSP for parameter estimation are also compared with three cases of naïve/common-sense sensor placements. The three commonsense cases include: (c1) uniform along the whole structure, (c2) uniform along the height of the tower, and (c3) locations obtained by Kammer's method [20] which maximizes the linear independence of mode shapes. The first 8 modes of the structure are considered in the application of Kammer's method. The entropy values for these three cases are compared with the OSP results for parameter estimation in Fig. 12. It can be observed that the entropy from case c2 (uniform along the tower) is close to OSP results but cases c1 and c3 provide inferior results.

4.4. Cost consideration

The previous section provided OSP results for parameter estimation without consideration of cost, where sensor locations were provided sequentially for a known number of sensors. This section provides the OSP results where sensor installation cost can be drastically different at different locations such as offshore wind turbine structures. Using Eq. (21), the cost and benefit of this case are calculated. The reference minimum information entropy (H_{ref}) is calculated by assuming 8 sensors. The reason behind this choice is the tradeoff between information entropy and cost. Assuming a higher number of sensors would force the weight factor for balancing cost and benefit to be infinitesimal. In this section, the cost-benefit objective function (Eq. (22)) is minimized with a weight factor of $w = 0.55$. The weight factor value is chosen such that it gives a balanced result. The SSP method is implemented, and its results are compared with those from the exhaustive search. The OSP analysis is performed assuming a spatial correlation length of $\lambda = 5$ under both lateral and torsional loads.

The installation cost for one sensor is assumed to be \$10,000 at underwater locations, \$5000 within the splash zone, and linearly increasing from \$1000 to \$2000 along the tower height. The sensor installation cost is shown in Fig. 13. Furthermore, the price of each sensor is assumed to be \$500, which is constant and is added to the installation cost. Fig. 14 shows the cost-benefit objective function of

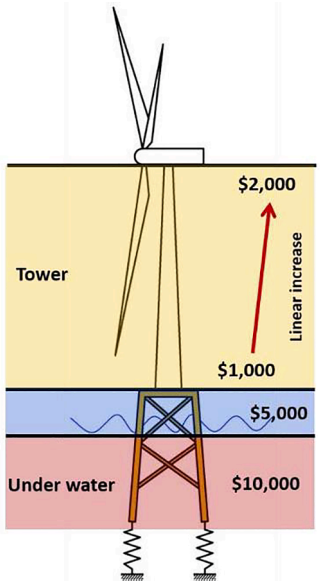

Fig. 13. Comparing three common-sense configurations with SSP results for parameter estimation.

all 4.613029×10^6 candidate sensor configurations using exhaustive search, where the results are grouped based on the number of the sensors in each candidate configuration and sorted in ascending order based on the value of the objective function. It can be seen that the objective function (f) of Eq. (22) within each group of sensors can be reduced drastically by optimal sensor placement, which highlights the importance and value of OSP. The red dots represent the best configuration within each group of sensors. The best configuration for the considered weight of $w = 0.55$ is when 2 sensors are used, which provides the lowest value of the objective function. It is worth noting that the results are sensitive to the weight between cost and benefit, w, in the objective function. Fig. 15 shows the optimum sensor configurations for each number of sensors. It can be observed that cost consideration slightly moves the optimal locations closer to the bottom of the tower where the installation cost is low. A smaller weight factor would reduce the weight on information entropy and increase the weight on cost, which results in sensors being pulled down until all of them are placed in the minimum cost locations for the extreme case of $w = 0$. The accuracy of the OSP results from SSP and the exhaustive search is compared in Fig. 16. The results confirm the previous conclusion about the accuracy and efficiency of SSP for the case of using an objective function with cost consideration.

Table 1 compares the effectiveness of the OSP when estimating parameters using 1-sensor to 5-sensor configurations. SSP search method results are used for comparison. A u value that is more than zero shows that using this framework is beneficial.

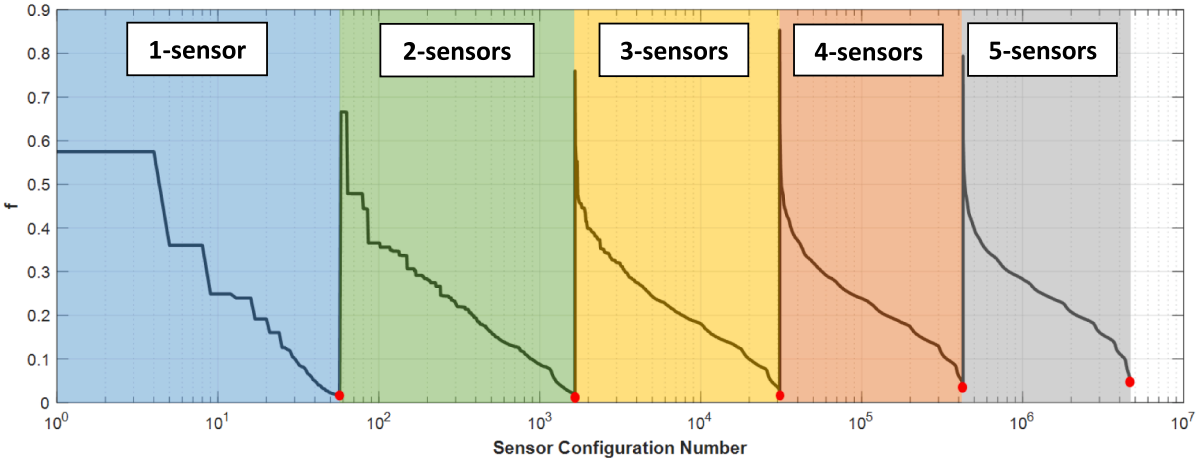

Fig. 14. Sensor installation cost.

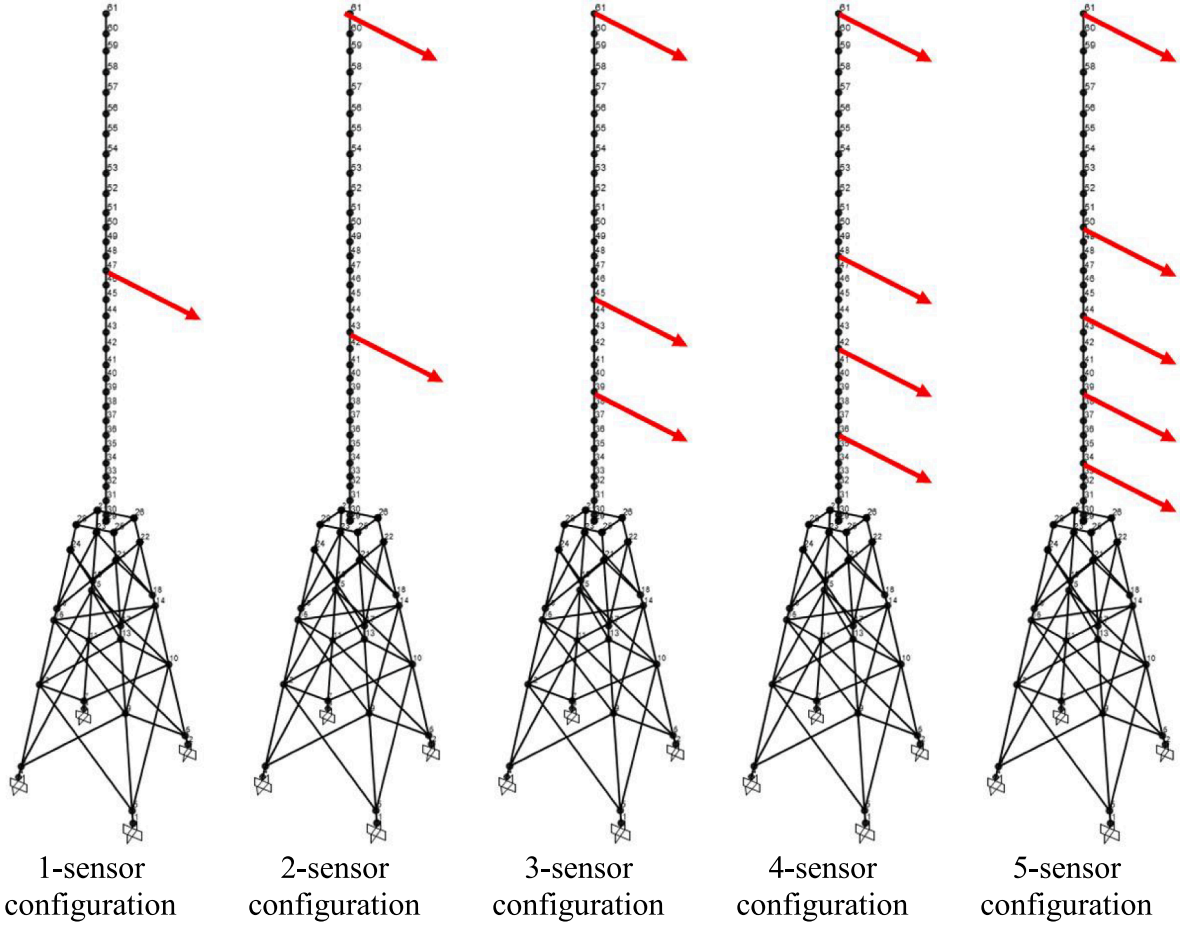

Fig. 15. Sorted objective function f for 1–5 sensor configurations.

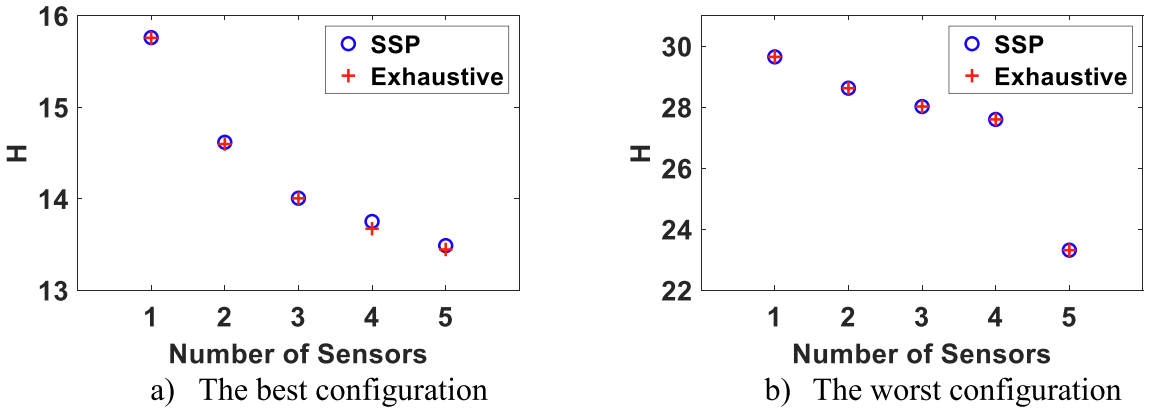

Fig. 16. Optimal sensor configuration results for different number of sensors with the consideration of installation cost.

Table 1
Comparing the measure of effectiveness for parameter estimation for different number of sensors.

	1-sensor	2-sensor	3-sensor	4-sensor	5-sensor
u	0.88	0.96	1.00	1.01	0.73

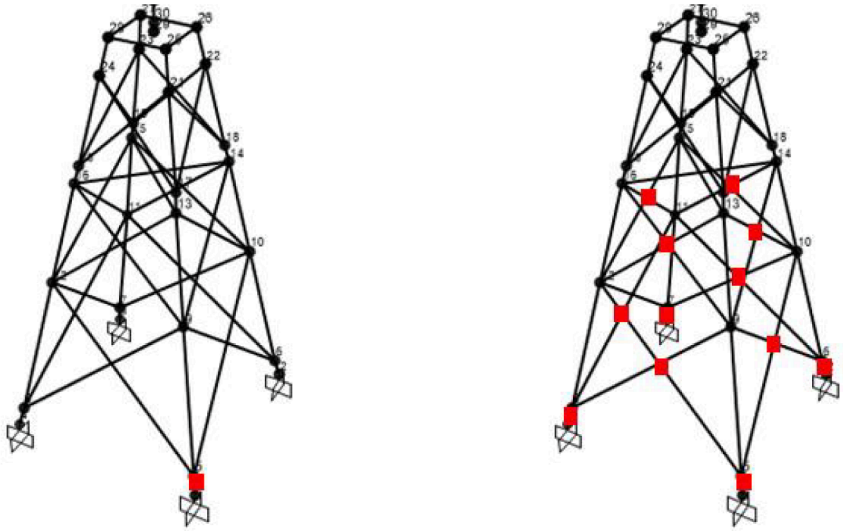

Fig. 17. Strain estimation locations.

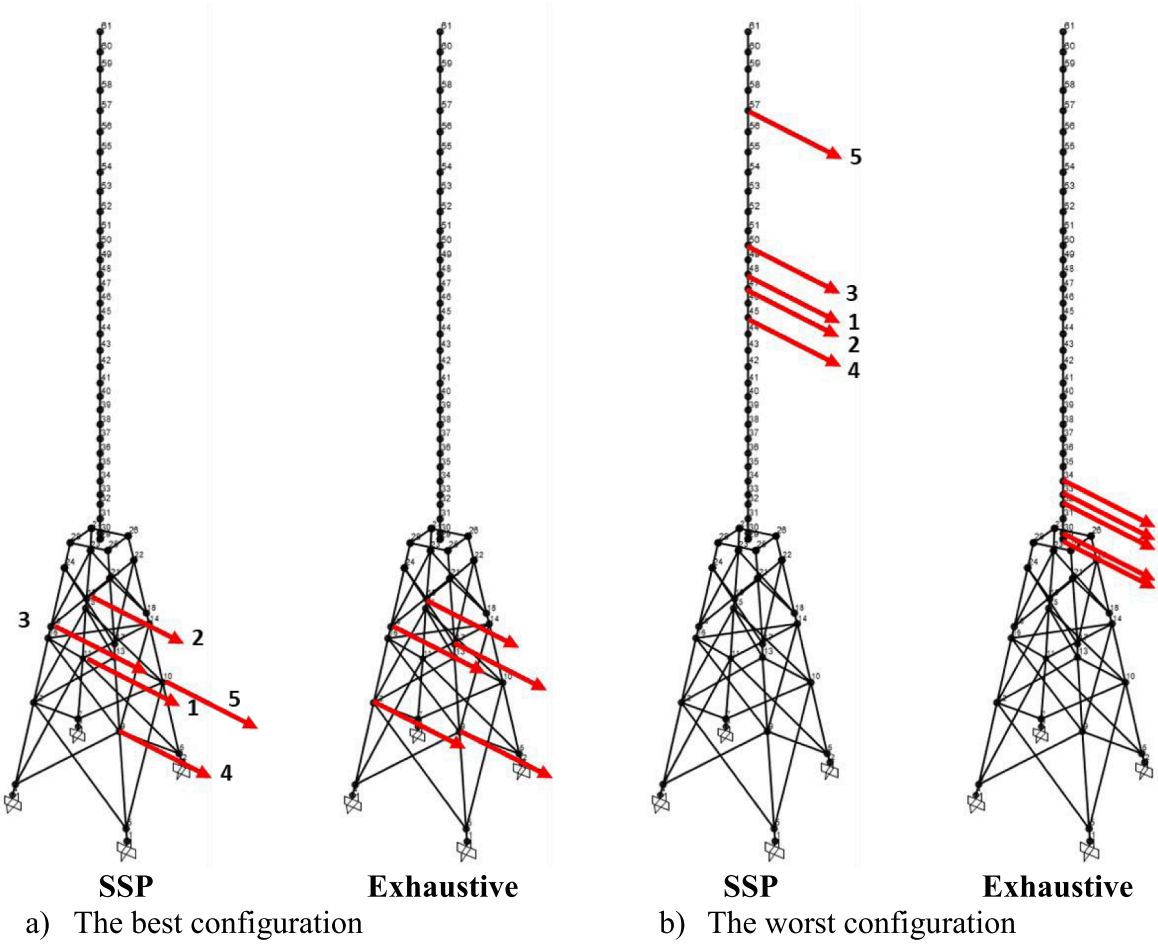

Fig. 18. Comparing OSP results for strain estimation at a single hotspot using SSP and exhaustive methods.

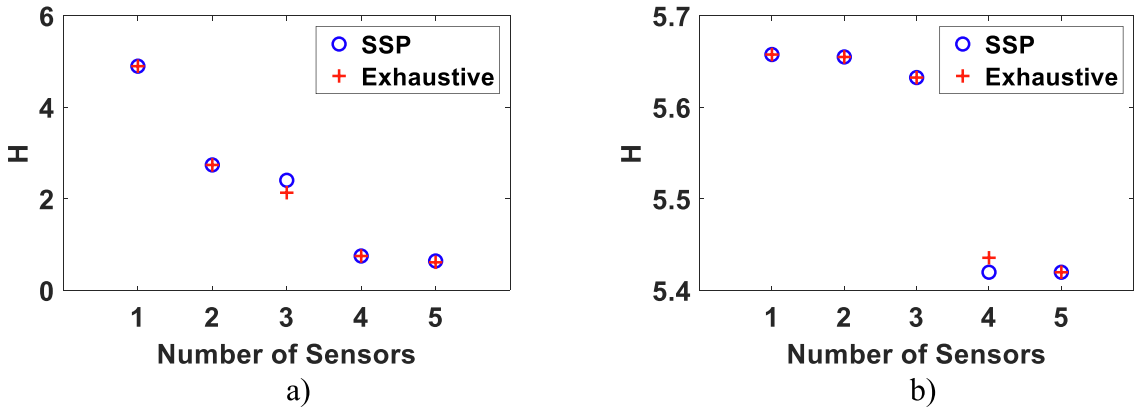

Fig. 19. The information entropy of OSP results for strain estimation at a single hotspot using SSP and exhaustive methods for a) the best configurations; b) the worst configurations.

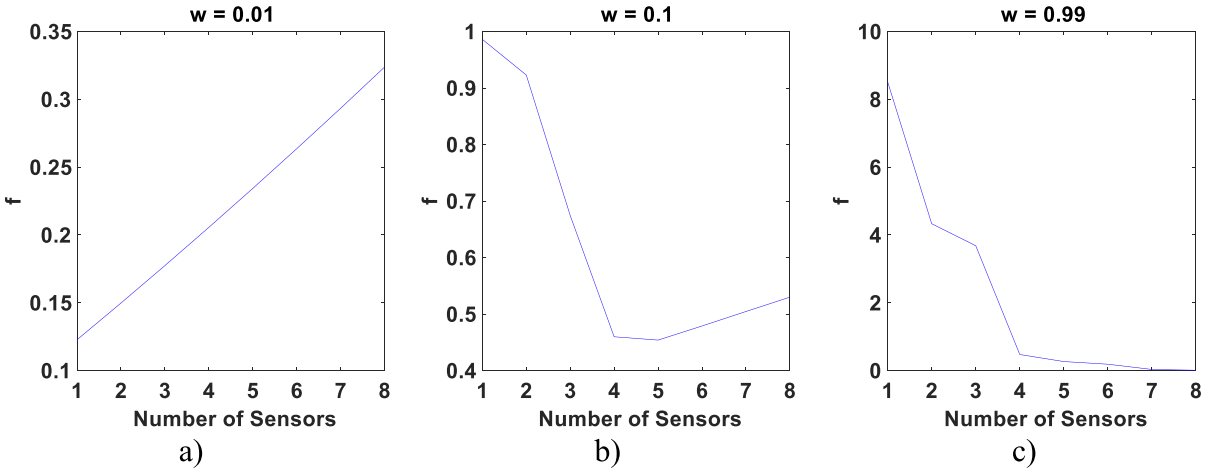

Fig. 20. The objective function of OSP results for strain estimation at a single hotspot using the SSP method for the best configurations.

5. OSP results for strain estimation

Two OSP problems are studied in this section, as shown in Fig. 17, for estimating the axial strain at different fatigue hotspots, namely (1) one location at the bottom of the jacket just above the support, since lower joints are more prone to fatigue and (2) at twelve locations, middle of eight diagonal members and four elements at the bottom of the jacket. Both problems are solved with and without cost consideration. The first five vibration modes of the structure, as shown in Fig. 2, are considered in this study. The prior knowledge about the modal coordinate in Eq. (10) is assumed to be Gaussian with a large $\mathbf{\Sigma}_{pr} = 10^{13}$, which implies unknown prior knowledge similar to the assumption of uniform distribution. The covariance of strain prediction error is postulated as $\mathbf{\Sigma}_{\epsilon} = 10^{-1}$ at all locations.

5.1. OSP for estimating strains at one location

Case 1: No cost consideration

Using the formulation presented in Sections 2.2, 2.3, and 2.4.2 of this paper, OSP is found using the SSP algorithm and the exhaustive search for a 5-sensor configuration. Prediction error correlation is considered using a correlation length of $\lambda = 5$. Fig. 18 depicts OSP results together with the worst sensor placements for 5-sensor configurations. The information entropy of OSP results for strain estimation using SSP and exhaustive search are compared in Fig. 19 for the best and worst sensor configurations.

This investigation confirms the previous observation about the accuracy of the SSP method, which states that SSP provides near-optimal solutions for the OSP problem. It is worth noting that the order of placing sensors is available only when using the SSP and can be interpreted as the relative importance of each sensor. The exhaustive search does not automatically provide such ordering. In Fig. 19, it is seen that adding the fifth sensor provides little information compared to the first four sensors. Fig. 19 shows the accuracy of the SSP method, as well as the usefulness of the OSP algorithm by comparing the information entropy of the best and worst

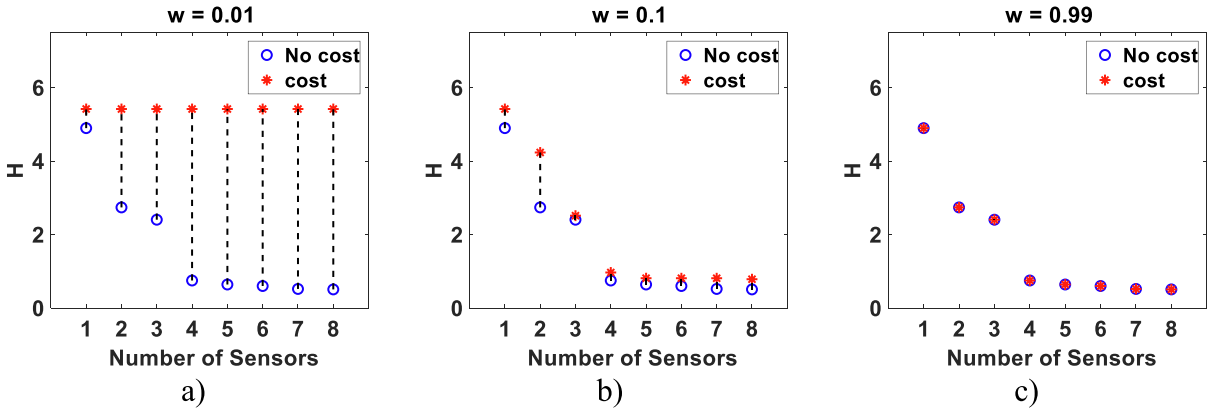

Fig. 21. The difference in information entropy of OSP results for strain estimation at a single hotspot with and without cost consideration.

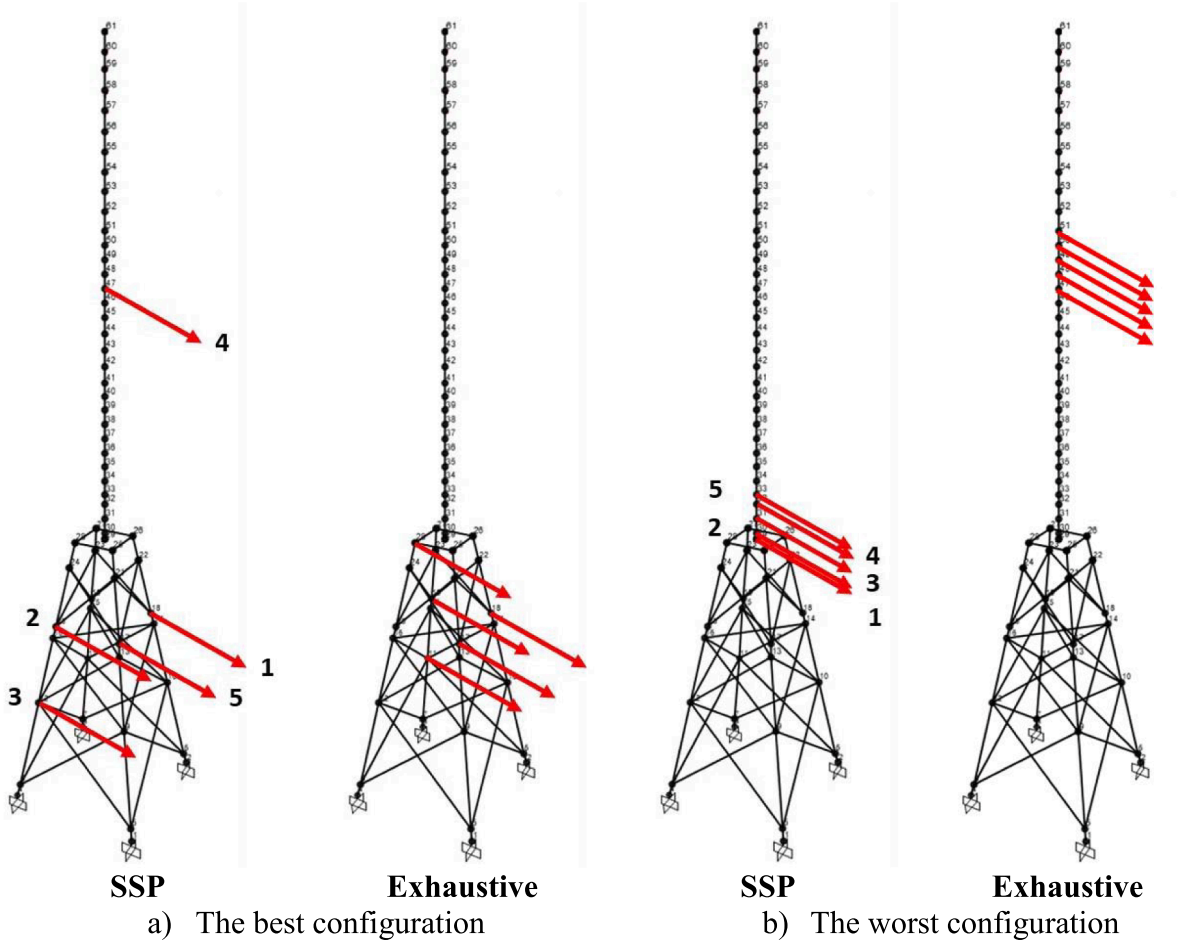

Fig. 22. Comparing results of OSP for strain estimation at 12 hotspots using SSP and exhaustive methods.

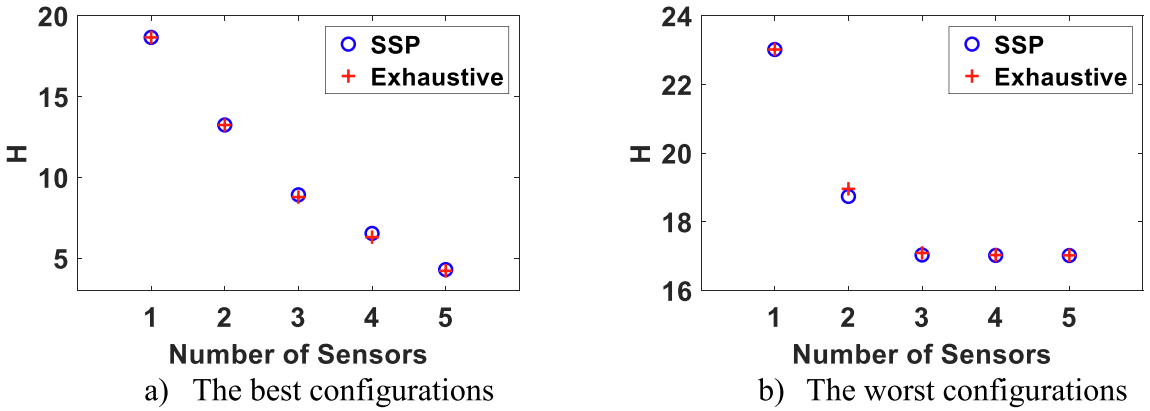

Fig. 23. The information entropy of OSP results for strain estimation at 12 hotspots using SSP and exhaustive methods for a) the best configurations; b) the worst configurations.

Table 2
Comparing the measure of effectiveness for estimating strains at one and twelve locations.

	1-sensor	2-sensor	3-sensor	4-sensor	5-sensor
1 location	0.15	1.06	1.34	6.20	7.42
12 locations	0.23	0.41	0.91	1.61	2.96

configurations. Although Fig. 18b shows that SSP and exhaustive search provide different worst sensor configurations, Fig. 19b shows that the resultant information entropies are generally similar.

Case 2: OSP with cost consideration

To account for the cost in the OSP, a multi-objective optimization is employed by varying the weight factor between the information entropy and cost in Eq. (22). Similar to section 4.4, the reference minimum information entropy (H_{ref}) is calculated by assuming 8 sensors. Weight $w = 0$ indicates the case where the OSP result is dominated by the cost and $w = 1$ is the other extreme where information entropy dominates the solution. Three weight factors of 0.01, 0.1, and 0.99 are used. These weight values are chosen to show two extreme and one balanced scenarios. Note that $w = 0.55$ was a balanced case for parameter estimation. However, for strain estimation, based on the value of information entropy and cost, $w = 0.1$ is found to be more balanced. In this case, 1-sensor to 8-sensor configurations are investigated. The SSP algorithm is used, and prediction error correlation is considered using a correlation length of $\lambda = 5$. The values of objective functions are displayed in Fig. 20 for different sensor numbers, and the three considered weights. As shown in Fig. 20a, the best setup that minimizes the objective function for $w = 0.01$ is a 1-sensor configuration, and the objective function is monotonically increasing by adding more sensors. This is due to the high weight of the cost component compared to the normalized benefit. For the case of $w = 0.1$, the objective function is not monotonically increasing or decreasing and has a minimum at 5 sensors due to the balance between the values of cost and information, as shown in Fig. 20b. Therefore, the OSP, which minimizes the objective function, has 5 sensors. The last scenario with $w = 0.99$ shows control of the information entropy over the OSP results. The objective function, in this case, is monotonically decreasing like the case where cost is not considered. The best sensor setup is an 8-sensor configuration where the objective function is minimum. Fig. 21 shows the corresponding information entropy of the OSP designs for different sensor setups with the three considered weights of 0.01, 0.1, and 0.99 together with the case when the cost is not considered. In this figure, the dashed line provides a visual measure to show the difference between information entropy when the cost is considered and when it is not. It can be seen that this difference is the largest for $w = 0.01$ while it becomes negligible for $w = 0.99$. Furthermore, in Fig. 21(a), where the weight of information entropy is very low, it remains almost constant by adding sensors. This is because the sensors are added in locations with the minimum cost, which in this particular structure coincide with the least informative locations (See Fig. 18b using exhaustive search). However, adding more sensors would result in a decrease in information entropy eventually. By increasing the weight of information entropy in the objective function, the discrepancy between cost and no-cost cases diminishes. The weight factor should be chosen to maintain a balance between cost and information entropy and such that not much information is lost when the cost is considered. It is worth mentioning that for the case $w = 0.1$, the results in Fig. 21(b) suggest that the information gained by adding more than 5 sensors at their optimal locations is not significant to justify the cost from the additional sensors.

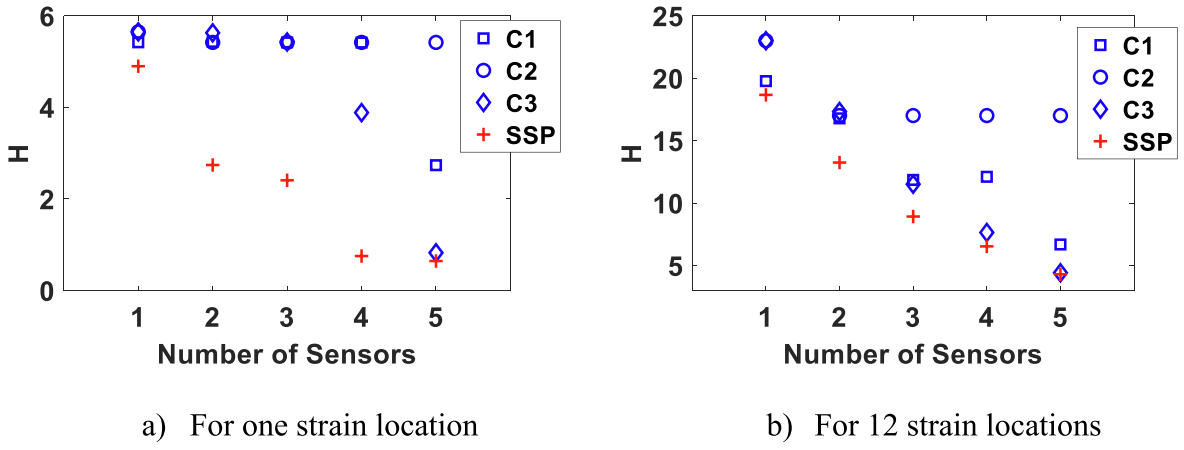

Fig. 24. The difference in information entropy of OSP results for strain estimation at 12 hotspots with and without cost consideration.

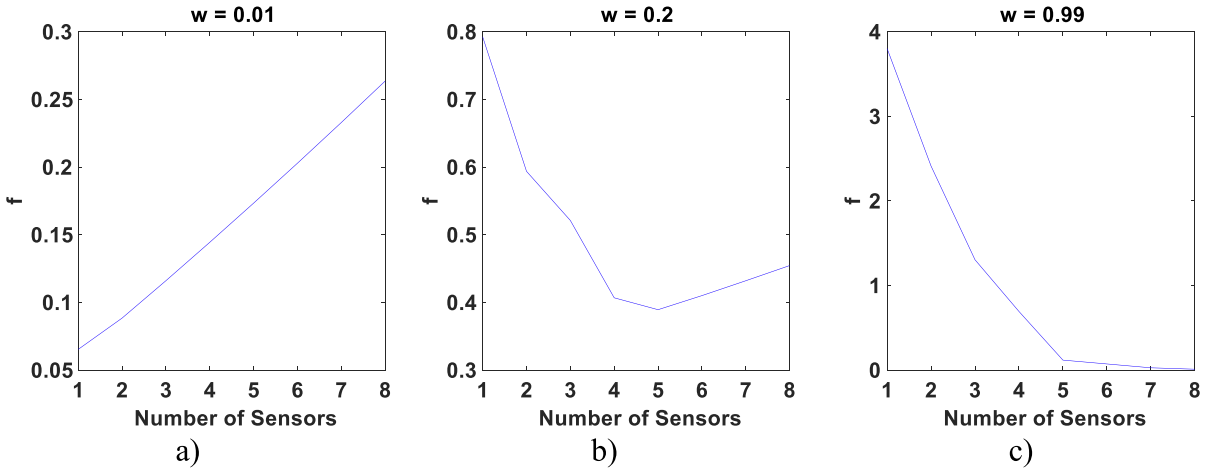

Fig. 25. Comparing three common-sense configurations with SSP results for strain estimation.

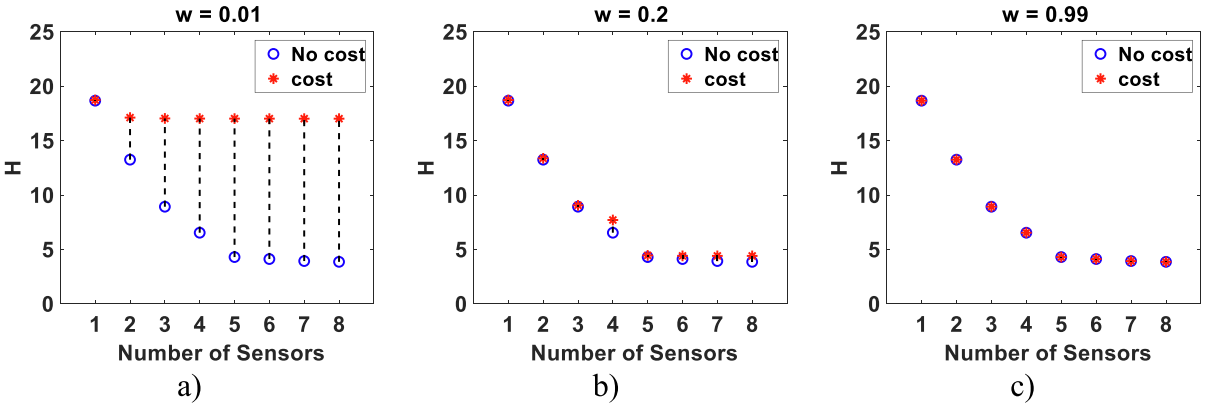

Fig. 26. The objective function of OSP results for strain estimation at 12 hotspots using the SSP method for the best configurations.

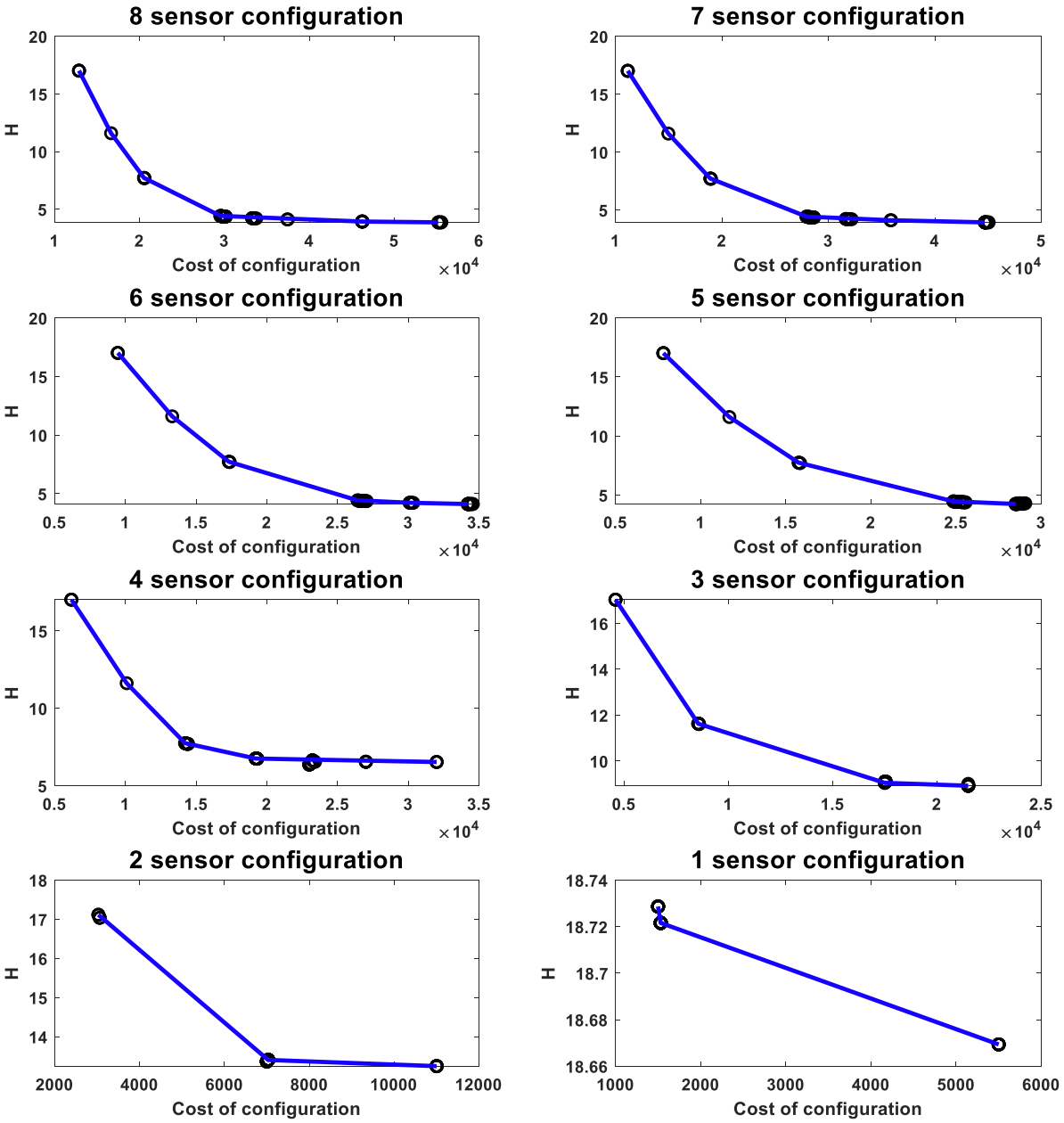

Fig. 27. Pareto plot (cost vs information entropy) for 1–8 sensor configurations.

5.2. OSP for estimating strains in twelve hotspot locations

Previous studies have shown that X joints are more susceptible to fatigue compared to K joints [47]. Thus, the X joints located at the middle of eight lower members, as well as the bottom of the four jacket legs, are chosen as fatigue hotspots for strain estimation, as shown in Fig. 17b. OSP is performed with and without cost constraint, assuming a $\lambda = 5$ correlation length and utilizing both SSP and exhaustive search algorithms.

Case 1: OSP without cost consideration

The same framework as that of Section 5.1 is used here. Fig. 22 illustrates the best and worst configurations for a 5-sensor configuration. There are some discrepancies in the location of sensors for both the best and the worst cases using the two search methods. However, the information entropy values shown in Fig. 23 are very similar. It can be seen that the differences between the

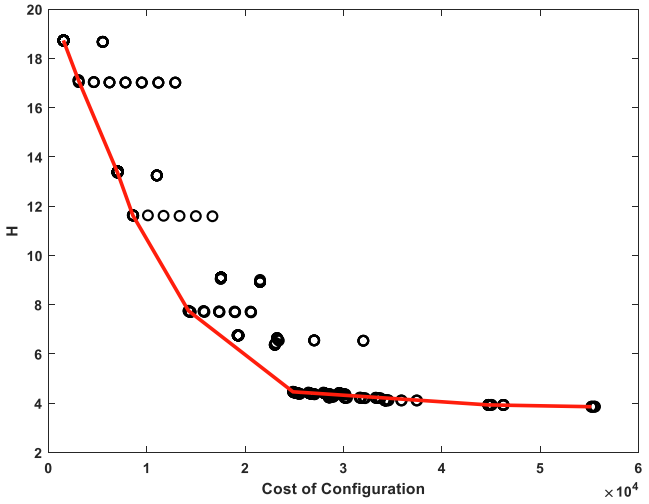

Fig. 28. Pareto plot (cost vs. information entropy) for all sensor configurations.

Table 3
Pareto solutions at different levels of information entropy.

Information entropy	H > 18	16 < H < 18	12 < H < 14	10 < H < 12	6 < H < 8	4 < H < 6
# of Sensors	1 sensor	2 sensors	2 sensors	3 sensors	4 sensors	5 sensors
Cost	$1500	$3031	$7000	$8562	$14,218	$24,843

two methods are minor in all cases, and the SSP is preferred due to its lower computational cost.

Table 2 compares the effectiveness of the OSP when estimating strains at one location and 12 locations using 1-sensor to 5-sensor configurations. SSP search method results are used for comparison. Table 2 shows that by increasing the number of strain estimation locations, the effectiveness of OSP decreases, especially for the cases with a higher number of sensors. This shows the importance of using OSP when the number of strain estimation locations is small. An intuitive explanation for this observation is that when more QoIs are estimated, every DOFs of the structure potentially contains more information on some of the QoIs, and the relative importance between DOFs decreases, i.e., the effectiveness of OSP decreases.

In the case of OSP for strain estimation, the entropy from OSP is compared with the same three cases of naïve/common-sense sensor placements, i.e., (c1) uniform along the whole structure, (c2) uniform along the height of the tower, and (c3) locations obtained by Kammer's method [20] considering the first 8 modes. The entropy values for these three cases are compared with the OSP results for strain estimation (1 location and 12 locations) in Fig. 24. It can be observed that in general, the commonsense cases are non-optimal while there are instances (e.g., 5 sensor setup) that c3 sensor configuration gets close to the optimal solution.

Case 2: OSP with cost consideration

In this case, OSP for strain estimation is performed considering sensor configuration cost. Similar to sections 4.4 and 5.1, the reference minimum information entropy (H_{ref}) is calculated by assuming 8 sensors. Three weight factors of 0.01, 0.2, and 0.99 are considered in the cost-benefit objective function of Eq. (22). The balanced weight factor ($w = 0.2$) is chosen to give a balanced result, and it is different compared to section 5.1 ($w = 0.1$) as the information entropy, and accordingly, the normalized benefit of configurations are different. Due to the high computational cost of exhaustive search and the confirmed accuracy of SSP, only the SSP method is implemented in this section. Fig. 25 shows the objective function (for OSP results) as a function of different number of sensors under three considered weight factors. Similar to Section 5.1, the best configuration for $w = 0.01$ is a 1-sensor configuration, for $w = 0.2$ is a 5-sensor configuration, and for $w = 0.99$ is an 8-sensor configuration. Fig. 26 illustrates the difference between information entropy when the cost is considered and when the cost is not considered. As expected, the differences between the entropy of with/out cost are the most when w is small and become negligible for $w = 0.99$.

To further investigate the effects of weight factors, a Pareto front study is performed, and the OSP is repeated considering 50 different weight factors ranging from 0 to 1 with intervals of 0.0204 and 1-sensor to 8-sensor configurations, i.e., a total of $50 \times 8 = 400$ OSP optimizations. Fig. 27 shows the Pareto front plots of OSP results for each number of sensors. The Pareto front plot includes solutions that are optimal, and no objective can be improved without sacrificing at least one other objective. This study is a multi-objective optimization with information entropy and cost as its objectives. The black circles correspond to OSP results using the considered 51 different weight factors. The blue line provides the values of cost and information entropy for different OSP and shows the tradeoff between them as their weight in the objective function varies. There are exactly 50 black circles in each plot; however, the

information entropy and cost of some of the configurations with different weight factors are the same resulting in the black circles being overlapped. Fig. 27 shows that by increasing the number of the sensors, as more configurations are available, there are more Pareto front solutions at different levels of entropy. For example, for 1-sensor configuration 50 different weight factors resulted in only three levels of information entropy, one high, one balanced, and one low. For 8 sensors, 8 levels are achieved. By means of these plots, the decision-maker can consider the required cost to achieve a certain level of information entropy or determine the amount of accuracy that can be achieved for a specific budget.

The information of the eight subplots in Fig. 27 is presented and condensed in a Pareto plot as Fig. 28. This plot can help to optimize the number of sensors as well as optimize the weight factor. The black circles are clustered in different levels of information entropy. In each cluster, there are configurations with different numbers of sensors and different weight factors overlapping but, there is only one configuration with minimum cost. This configuration is interpreted as the Pareto optimal configuration. For example, at the entropy level of ~12, there are 12 different configurations fitted (with 6 distinct circles visible). The configurations include 3 to 8 sensors, and with weights varying between 0.0612 and 0.1837, and the Pareto solution (least cost at a constant entropy level) is the one with 3 sensors and $w = 0.1837$. The Pareto solutions are connected with the red line. Every point on this line denotes the best configuration under the corresponding cost constraint, i.e., the information entropy cannot be decreased further without increasing the budget. The Pareto solutions are listed in Table 3. Fig. 28 and Table 3 could help the decision-makers with the OSP design, including the number of sensors given a budget, without a need to concern with the weight factor in the objective function.

6. Conclusion

This paper has formulated and evaluated an information theory-based OSP framework for parameter estimation and strain estimation considering sensor configuration cost. The OSP framework for parameter estimation requires the input information, while the OSP framework for strain estimation is an output-only method. The approach is evaluated numerically when applied to a realistic model of an offshore wind turbine. A computationally efficient approach, the SSP method, which is a combination of FSSP and BSSP methods, is employed to solve the OSP problem and is compared with the exhaustive search approach. The results are analogous to optimal configurations from the exhaustive search. The proposed optimization framework accounts for the sensor configuration cost on the structure. The sensor configuration cost is the summation of sensor installation cost, which is defined unevenly based on the location and sensor cost, which is constant. A cost-benefit objective function is defined and has been used in this study to account for both information entropy and cost constraint. In the objective function, a weight factor is used to balance the importance of information entropy versus cost. The OSP results are found to be sensitive to the weight factor, and thus, a Pareto front study is performed for different weight factors and different numbers of sensors. The Pareto plots can help the decision-makers to quantify the required cost to achieve a certain level of information entropy or alternatively determine the amount of accuracy/entropy that can be achieved for a specific budget.

Declaration of Competing Interest

The authors declare that they have no known competing financial interests or personal relationships that could have appeared to influence the work reported in this paper.

Acknowledgments

The authors acknowledge partial support of this study by the National Science Foundation grant 1903972, Bureau of Safety and Environmental Enforcement (BSEE), U.S. Department of the Interior, Washington, D.C., under Contract 140E0119C0003, and Massachusetts Clean Energy Center under AmplifyMass program. The opinions, findings, and conclusions expressed in this paper are those of the authors and do not necessarily represent the views of the sponsors and organizations involved in this project.

References

[1] IEA. Offshore Wind Outlook 2019: International Energy Agency; 2019. Available from: <https://www.iea.org/reports/offshore-wind-outlook-2019>.
[2] O. Adedipe, F. Brennan, A. Kolios, Corrosion fatigue load frequency sensitivity analysis, Mar. Struct. 42 (2015) 115–136.
[3] F. Brennan, I. Tavares, Fatigue design of offshore steel mono-pile wind substructures, Proc. Inst. Civil Eng.-Energy 167 (4) (2014) 196–202.
[4] B. Moaveni, System and damage identification of civil structures: UC San Diego, 2007.
[5] Guidelines for Structural Health Monitoring for Offshore Wind Turbine Towers & Foundations, 2017. Report No.: 16-1036.
[6] I. Behmanesh, B. Moaveni, Probabilistic identification of simulated damage on the Dowling Hall footbridge through Bayesian finite element model updating, Struct. Control Health Monit. 22 (3) (2015) 463–483.
[7] J.L. Beck, L.S. Katafygiotis, Updating models and their uncertainties. I: Bayesian statistical framework, J. Eng. Mech. 124 (4) (1998) 455–461.
[8] J.L. Beck, S.-K. Au, Bayesian updating of structural models and reliability using Markov chain Monte Carlo simulation, J. Eng. Mech. 128 (4) (2002) 380–391.
[9] J.L. Beck, K.-V. Yuen, Model selection using response measurements: Bayesian probabilistic approach, J. Eng. Mech. 130 (2) (2004) 192–203.
[10] I. Behmanesh, B. Moaveni, C. Papadimitriou, Probabilistic damage identification of a designed 9-story building using modal data in the presence of modeling errors, Eng. Struct. 131 (2017) 542–552.
[11] H. Sohn, K.H. Law, A Bayesian probabilistic approach for structure damage detection, Earthquake Eng. Struct. Dyn. 26 (12) (1997) 1259–1281.
[12] M. Song, S. Yousefianmoghadam, M.-E. Mohammadi, B. Moaveni, A. Stavridis, R.L. Wood, An application of finite element model updating for damage assessment of a two-story reinforced concrete building and comparison with lidar, Struct. Health Monit. 17 (5) (2018) 1129–1150.
[13] K.-V. Yuen, J.L. Beck, S.K. Au, Structural damage detection and assessment by adaptive Markov chain Monte Carlo simulation, Struct. Control Health Monit. 11 (4) (2004) 327–347.
[14] G. Capellari, Optimal design of sensor networks for structural health monitoring: Politecnico Di Milano, 2018.

[15] C. Papadimitriou, Optimal sensor placement methodology for parametric identification of structural systems, J. Sound Vib. 278 (4-5) (2004) 923–947.
[16] G. Heo, J. Jeon, An experimental study of structural identification of bridges using the kinetic energy optimization technique and the direct matrix updating method, Shock Vib. 2016 (2016) 1–13.
[17] G. Heo, M.L. Wang, D. Satpathi, Optimal transducer placement for health monitoring of long span bridge, Soil Dyn. Earthquake Eng. 16 (7-8) (1997) 495–502.
[18] N. Imamovic, Model validation of large finite element model using test data, 1998.
[19] D.C. Kammer, Sensor placement for on-orbit modal identification and correlation of large space structures, J. Guid., Control, Dyn. 14 (2) (1991) 251–259.
[20] D.C. Kammer, Optimal sensor placement for modal identification using system-realization methods, Jo. Guid., Control, Dyn. 19 (3) (1996) 729–731.
[21] P.H. Kirkegaard, R. Brincker, On the optimal location of sensors for parametric identification of linear structural systems, Mech. Syst. Sig. Process. 8 (6) (1994) 639–647.
[22] F.E. Udwadia, Methodology for optimum sensor locations for parameter identification in dynamic systems, J. Eng. Mech. 120 (2) (1994) 368–390.
[23] C. Yang, ZiXing Lu, An interval effective independence method for optimal sensor placement based on non-probabilistic approach, Sci. China Technol. Sci. 60 (2) (2017) 186–198.
[24] E. Heredia-Zavoni, L. Esteva, Optimal instrumentation of uncertain structural systems subject to earthquake ground motions, Earthquake Eng. Struct. Dyn. 27 (4) (1998) 343–362.
[25] E. Heredia-Zavoni, R. Montes-Iturrizaga, L. Esteva, Optimal instrumentation of structures on flexible base for system identification, Earthquake Eng. Struct. Dyn. 28 (12) (1999) 1471–1482.
[26] E.B. Flynn, M.D. Todd, A Bayesian approach to optimal sensor placement for structural health monitoring with application to active sensing, Mech. Syst. Sig. Process. 24 (4) (2010) 891–903.
[27] C.E. Shannon, A mathematical theory of communication, Bell Syst. Tech. J. 27 (3) (1948) 379–423.
[28] C. Papadimitriou, J.L. Beck, S.-K. Au, Entropy-based optimal sensor location for structural model updating, J. Vib. Control 6 (5) (2000) 781–800.
[29] K.-V. Yuen, L.S. Katafygiotis, C. Papadimitriou, N.C. Mickleborough, Optimal sensor placement methodology for identification with unmeasured excitation, J Dyn Sys, Meas, Control 123 (4) (2001) 677–686.
[30] P. Metallidis, G. Verros, S. Natsiavas, C. Papadimitriou, Fault detection and optimal sensor location in vehicle suspensions, J. Vib. Control 9 (3-4) (2003) 337–359.
[31] C. Papadimitriou, Pareto optimal sensor locations for structural identification, Comput. Methods Appl. Mech. Eng. 194 (12-16) (2005) 1655–1673.
[32] C. Papadimitriou, in: Optimal Sensor Placement for Response Reconstruction in Structural Dynamics. Model Validation and Uncertainty Quantification, Springer, 2020, pp. 205–210.
[33] D.V. Lindley, On a measure of the information provided by an experiment, Ann. Math. Stat. 27 (4) (1956) 986–1005.
[34] S. Kullback, R.A. Leibler, On information and sufficiency, Ann. Math. Stat. 22 (1) (1951) 79–86.
[35] C. Papadimitriou, G. Lombaert, The effect of prediction error correlation on optimal sensor placement in structural dynamics, Mech. Syst. Sig. Process. 28 (2012) 105–127.
[36] M.M. Abdullah, A. Richardson, J. Hanif, Placement of sensors/actuators on civil structures using genetic algorithms, Earthquake Eng. Struct. Dyn. 30 (8) (2001) 1167–1184.
[37] H. Bedrossian, S. Masri, in: Optimal Placement of Sensors and Shakers for Modal Identification. Computational Stochastic Mechanics, Millpress, Rotterdam, 2003, p. 5357.
[38] C. Papadimitriou, edi., Applications of genetic algorithms in structural health monitoring, in: Proc 5th World Congress on Computational Mechanics, Vienna, Austria, 2002.
[39] L. Yao, W.A. Sethares, D.C. Kammer, Sensor placement for on-orbit modal identification via a genetic algorithm, AIAA J. 31 (10) (1993) 1922–1928.
[40] M.-S. Nabiyan, F. Khoshnoudian, B. Moaveni, H. Ebrahimian, Mechanics-based model updating for identification and virtual sensing of an offshore wind turbine using sparse measurements, Struct. Control Health Monit. 28 (2) (2021), https://doi.org/10.1002/stc.v28.210.1002/stc.2647.
[41] C. Papadimitriou, C.-P. Fritzen, P. Kraemer, E. Ntotsios, Fatigue predictions in entire body of metallic structures from a limited number of vibration sensors using Kalman filtering, Struct. Control Health Monitor. 18 (5) (2011) 554–573.
[42] M. Henkel, J. Häfele, W. Weijtjens, C. Devriendt, C.G. Gebhardt, R. Rolfes, Strain estimation for offshore wind turbines with jacket substructures using dual-band modal expansion, Mar. Struct. 71 (2020) 102731, https://doi.org/10.1016/j.marstruc.2020.102731.
[43] A. Iliopoulos, R. Shirzadeh, W. Weijtjens, P. Guillaume, D.V. Hemelrijck, C. Devriendt, A modal decomposition and expansion approach for prediction of dynamic responses on a monopile offshore wind turbine using a limited number of vibration sensors, Mech. Syst. Sig. Process. 68-69 (2016) 84–104.
[44] A. Iliopoulos, W. Weijtjens, D. Van Hemelrijck, C. Devriendt, Fatigue assessment of offshore wind turbines on monopile foundations using multi-band modal expansion, Wind Energy 20 (8) (2017) 1463–1479.
[45] A. Skafte, J. Kristoffersen, J. Vestermark, U.T. Tygesen, R. Brincker, Experimental study of strain prediction on wave induced structures using modal decomposition and quasi static Ritz vectors, Eng. Struct. 136 (2017) 261–276.
[46] M. Tarpø, B. Nabuco, C. Georgakis, R. Brincker, Expansion of experimental mode shape from operational modal analysis and virtual sensing for fatigue analysis using the modal expansion method, Int. J. Fatigue 130 (2020) 105280, https://doi.org/10.1016/j.ijfatigue.2019.105280.
[47] J. Häfele, C. Hübler, C.G. Gebhardt, R. Rolfes, A comprehensive fatigue load set reduction study for offshore wind turbines with jacket substructures, Renewable Energy 118 (2018) 99–112.
[48] J. Kullaa, Bayesian virtual sensing for full-field dynamic response estimation, Procedia Eng. 199 (2017) 2126–2131.
[49] J. Kullaa, Bayesian virtual sensing in structural dynamics, Mech. Syst. Sig. Process. 115 (2019) 497–513.
[50] T. Ercan, C. Papadimitriou, Optimal sensor placement for reliable virtual sensing using modal expansion and information theory, Sensors 21 (10) (2021) 3400.
[51] F. McKenna, OpenSees: a framework for earthquake engineering simulation, Comput. Sci. Eng. 13 (4) (2011) 58–66.
[52] S. Bhattacharya, Design of Foundations for Offshore Wind Turbines, Wiley, 2019.